Zootaxa 4061 (3): 201–226
http://www.mapress.com/j/zt/

Article

ISSN 1175-5326 (print edition)
ZOOTAXA
ISSN 1175-5334 (online edition)

http://doi.org/10.11646/zootaxa.4061.3.1
http://zoobank.org/urn:lsid:zoobank.org:pub:719E677E-45E4-40A1-BE1D-5030CFB421CD

A review of *Cordylus machadoi* (Squamata: Cordylidae) in southwestern Angola, with the description of a new species from the Pro-Namib desert

EDWARD L. STANLEY[1,7], LUIS M. P. CERÍACO[2,7], SUZANA BANDEIRA[3], HILARIA VALERIO[3], MICHAEL F. BATES[4] & WILLIAM R. BRANCH[5,6]

[1]*Department of Vertebrate Zoology and Anthropology, California Academy of Sciences, 55 Music Concourse Drive, San Francisco 94118, USA*

[2]*Museu Nacional de História Natural e da Ciência, Universidade de Lisboa, Rua da Escola Politécnica, 58, 1269-102 Lisbon, Portugal*

[3]*Instituto Nacional da Biodiversidade e Áreas de Conservação, Ministério do Ambiente de Angola, Centralidade do Kilamba, Rua 26 de Fevereiro, quarteirão Nimi ya Lukemi, edíficio Q11, 3º andar, Angola*

[4]*Department of Herpetology, National Museum, P.O. Box 266, Bloemfontein 9300, South Africa*

[5]*Port Elizabeth Museum, P.O. Box 13147, Humewood 6013, South Africa*

[6]*Research Associate, Department of Zoology, Nelson Mandela Metropolitan University, P.O. Box 77000, Port Elizabeth 6031, South Africa*

[7]*Department of Herpetology, Florida Museum of Natural History, Gainesville, FL, 32611, USA*

Corresponding author = Edward Stanley, email address estanley@calacademy.org

Abstract

The girdled lizard genus *Cordylus* is represented in Angola by two species, *Cordylus angolensis* and *C. machadoi*, separated from their nearest congeners by over 700 km. Here we describe a new species, *Cordylus namakuiyus* **sp. nov.**, endemic to the arid lowlands west of the southern Angolan escarpment. Phylogenetic analysis using three mitochondrial and eight nuclear genes shows that the low-elevation forms and the proximate, high-elevation species *C. machadoi* are genetically divergent and reciprocally monophyletic, and together form the earliest diverging lineage of the northern *Cordylus* clade. Morphological data, collected using computed tomography and traditional techniques (scalation and morphology), identify consistent phenotypic differences between these high- and low-elevation species and allows for a detailed description of the osteology and osteodermal arrangements of the new species. A series of 50 specimens, collected during the 1925 Vernay expedition to southwestern Angola and housed at the American Museum of Natural History, are assigned to the new species, although the identity of *Cordylus* from northern Namibia remains ambiguous and requires further investigation.

Key words: computed tomography, girdled lizard, Kaokoveld, molecular phylogeny, ontogeny, osteoderms, osteology

Resumo

Os largatos espinhosos das género *Cordylus* estão representados em Angola por duas espécies, *Cordylus angolensis* e *C. machadoi*, separados dos seus congéneres mais próximos por uma uma distância superior a 700 km. Neste artigo, descreve-se uma nova espécie, *Cordylus namakuiyus* **sp. nov.**, endémica do planícies áridas a oeste da escarpa sul de Angola. Análises filogenéticas com base em três genes mitocondriais e oito genes nucleares demonstram que as formas da zona de baixa elevação e a espécie vizinha que ocorre nas áreas mais elevadas, *C. machadoi*, são geneticamente divergentes e reciprocamente monofiléticas, e que juntas constítuem a linhagem divergente mais antiga do clado norte do género *Cordylus*. Dados morfológicos, recolhidos através de tomografia computacional e técnicas mais tradicionais (contagem de escamas e morfometria), identificam diferenças fenotípicas consistentes entre as espécies de baixa e alta elevação e permitem uma descrição detalhada da osteologia e distribuição dos osteodermos da nova espécie. Uma série de 50 espécimes, colectados na expedição de Vernay ao sudoeste de Angola em 1925, e actualmente depositados no American Museum of Natural History, são atribuídos à nova espécie, embora a identificação de um *Cordylus* do norte da Namibia permaneça ambígua e necessite de investigação mais detalhada.

Accepted by C. Siler: 26 Nov. 2015; published: 7 Jan. 2016

Introduction

The genus *Cordylus* Laurenti currently contains 21 recognized species, with distributional ranges from the Cape of Good Hope to southern Ethiopia, making it the most speciose and geographically widespread of the 10 cordylid genera (Stanley *et al.* 2011; Greenbaum *et al*., 2012). Recent phylogenetic work has revealed that *Cordylus* is divided into two latitudinally disjunct clades (Stanley *et al*., 2011). The southern clade, comprising nine species, is restricted to the southwestern quadrant of South Africa, from the inland Transkei in the east to the Northern Cape coast in the west (Branch, 1998; Mouton *et al*., 2014). The 12 species of the northern clade display a further biogeographic disjunction; the majority of species are found along the eastern escarpment, from South Africa to Ethiopia, while two isolated species, *Cordylus angolensis* (Bocage, 1895) and *Cordylus machadoi* Laurent, 1964, occur in southwestern Angola and northwestern Namibia.

Several studies have investigated the phylogenetic relationships of *Cordylus.* However, in all analyses, basal relationships within the northern clade were poorly resolved and topologically inconsistent. Stanley *et al*., (2011) recovered the southernmost species, *Cordylus vittifer* (Reichenow), as the earliest diverging lineage, whereas Greenbaum *et al.* (2012) and Nielsen and Colston (2014) identified the Angolan species, *C. machadoi*, as basal. Although the southern clade has been well studied (see Mouton *et al.*, 2014), knowledge of the distribution and diversity of *Cordylus* north of the subcontinent is patchy, with new species recently discovered in northern Malawi (*C. nyikae*, Broadley and Mouton 2000), northern Tanzania (*C. beraduccii*, Broadley and Branch, 2002) , northern Mozambique (*C. meculae*, Branch *et al*., 2005), and southeastern Democratic Republic of the Congo (*C. marunguensis,* Greenbaum *et al*., 2012). The Angolan species remain poorly known, with very little material available in museum collections. Despite extensive herpetological collecting in the 19th and early 20th centuries, large areas of Angola—particularly the inaccessible central and southeastern parts—were never properly surveyed (Marques 2015), and many of the specimens collected during earlier expeditions have been lost through neglect or calamity.

Cordylus angolensis (Bocage, 1895) was described from a single specimen from Caconda, Huíla Province, collected by José d'Anchieta, and housed in the Lisbon Museum, until it was destroyed in the 1978 fire. In the same paper, Bocage also identified two specimens housed in Sociedade de Geografia de Lisboa as the "widespread southern african *Zonurus* [*Cordylus*] *cordylus"* from Angola, though he noted that these specimens lacked precise locality information. Monard (1937) considered these specimens to be attributable to *C. vittifer*, although Loveridge (1944) considered this opinion untenable. The identity of these specimens remains a mystery, but the lack of suitable intervening habitat and sheer distance between the southern border of Angola and the known ranges of *C. cordylus* and *C. vittifer* (a geographic break of at least 700 km) makes the species assignments of Bocage and Monard unlikely.

Cordylus machadoi (Laurent, 1964) was originally described as a subspecies of *C. vittifer* on the basis of one male and a juvenile from Leba (1800 m above sea-level) on the western edge of the Bié region of the Angolan escarpment, in the vicinity of Sá da Bandeira (now Lubango), Huíla Province. The whereabouts of the holotype is currently unknown (though presumed to be in the Museu do Dundo, Dundo, Angola), while the juvenile paratype is housed at the Museum of Comparative Zoology (MCZ), Harvard University, Massachusetts. Small series of *C. machadoi* collected from 1971–2012 are housed in the National Museum of Namibia (NMN), Windhoek, Namibia, and the Ditsong (DM, museum specimen numbers = TM) and Port Elizabeth (PEM) museums in South Africa. The PEM material was collected during a collaborative South African-Angolan biodiversity initiative, and included both topotypic material of *C. machadoi* and a specimen from the ProNamib region of Angola (Huntley 2009). A collection of five *C. machadoi* from the Baynes and Otjihepa Mountains in northern Namibia, identified by D. G. Broadley (*personal communication*) was originally housed at the Namibian Department of Nature Conservation, although this material now appears to be lost. The American Museum of Natural History (AMNH) holds a collection of 55 *Cordylus*, collected during the 1925 Vernay Angola expedition. Fifty of these specimens are presently assigned to "*C. cordylus*" (locality "Angola") and five specimens from Mombolo in the Kwanza Sul Province of Angola are assigned to "*C. tropidosternum jonesi*". Charles M. Bogert recognised that the *C. cordylus* (Linnaeus) specimens did not agree with any *Cordylus* species known at that time and began writing a species description (Fig. 1), although this was never completed. Greenbaum *et al.* (2012) attributed three of the Mombolo individuals to *C. angolensis*, based on scale characters.

During a recent expedition to southwestern Angola, an international team, working with Angola's Instituto

Nacional de Biodiversidade e Areas de Conservation (INBAC), collected eight *Cordylus* from the rocky desert west of the southern Angolan escarpment (Fig. 2). These specimens prove to be morphologically and genetically distinct from the geographically proximate, high-elevation species *C. machadoi*. Herein, we investigate the phylogenetic position of southern Angolan *Cordylus*, discuss the hidden diversity within *C. machadoi* and describe a new species from the southwestern lowlands.

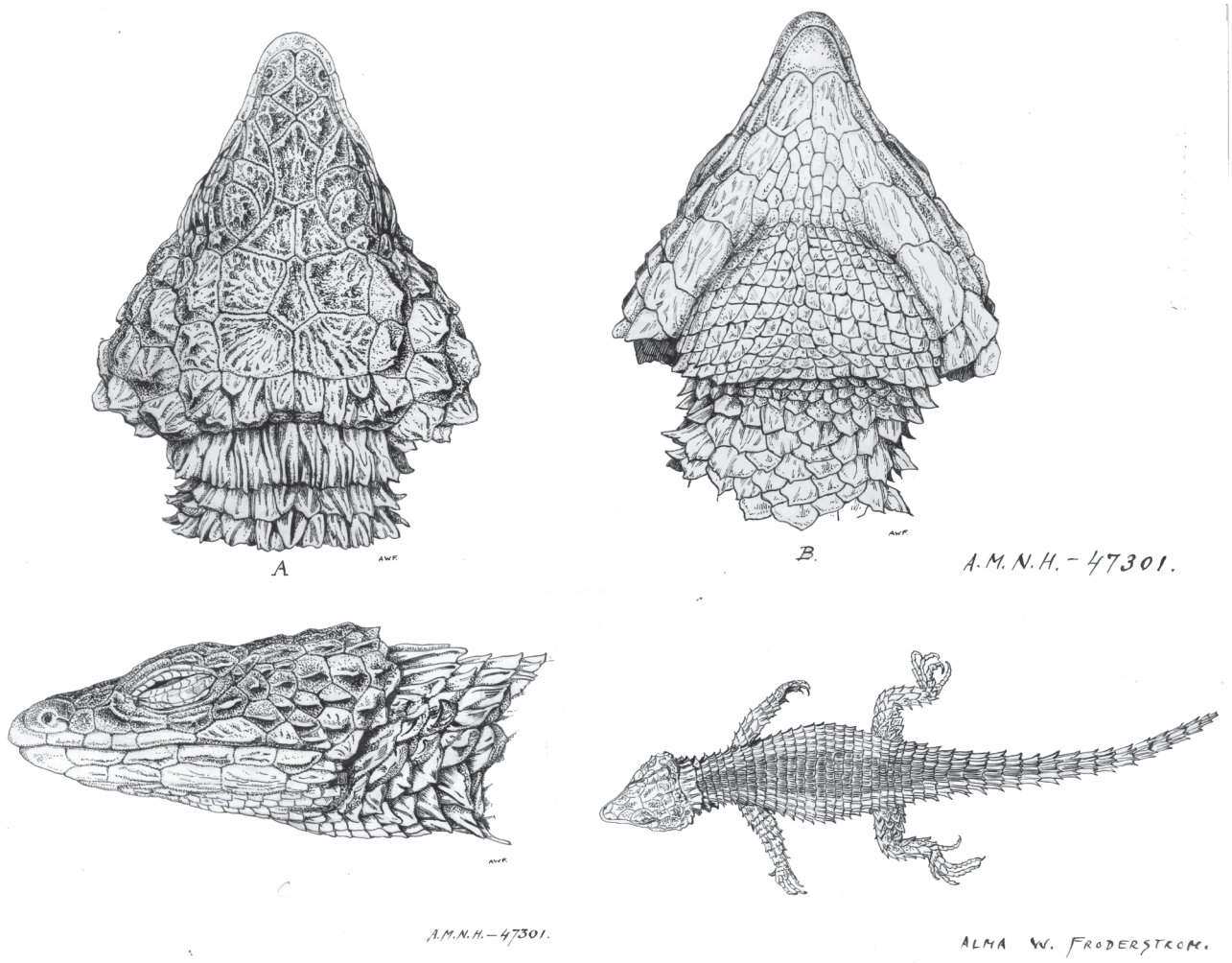

FIGURE 1. Head and body diagrams of *Cordylus* sp. (AMNH 47301, "Angola") from an unpublished species description by Charles M. Bogert, illustrated by Alma W. Froderstrom, reproduced with the permission of the Department of Herpetology at the American Museum of Natural History

Material and methods

Field work, sample collection, and specimen preservation. Specimens collected for this study were preserved in 10% buffered formalin in the field and transferred to 70% ethanol or 50% isopropanol at the conclusion of each expedition. Liver tissue was removed before formalin fixation and preserved in 95% ethanol. We also examined all available comparative *C. machadoi* material deposited in the MCZ, NMN, DM, and PEM collections, as well as the series of *Cordylus* incertae sedis from the AMNH (see supplementary data S1).

Sequence procurement and alignment. This study employed a dataset of eleven mitochondrial and nuclear genes. Sequences of six genes (16S, 12S, ND2, PRLR, Kif24 and MYH2) were obtained from GenBank for 17 species of *Cordylus* and two outgroup taxa, *Namazonurus campbelli* (FitzSimons) and *Ouroborus cataphractus* (Boie). Sequences for these same markers were produced for a further 12 specimens of Angolan *Cordylus*, and an additional five nuclear protein-coding genes were sequenced for the entire dataset (Table 1). All novel sequences were produced in the Centre for Comparative Genomics at CAS using the following methods: Genomic DNA was

isolated from ethanol-preserved liver or muscle tissue using Qiagen DNeasy Tissue Extraction Kits (Valencia, California, USA). Double-stranded PCR was used to amplify three mitochondrial (16S, 12S and ND2) and nine nuclear (R35, NKTR, KiF24, PRLR, MYH2, RAG1, CMOS and BDNF) genes, employing primers listed in Stanley *et al.* (2011) and Wiens *et al.* (2010). Amplification of 25µl PCR reactions was executed on Bio-Rad thermocyclers, beginning with an initial denaturation at 95˚C for 2 min followed by 95˚C for 35 s, annealing at 50˚C for 35 s, and extension at 72˚C for 150 s for 32 cycles for mitochondrial DNA and 34 cycles for nuclear DNA. Annealing temperatures were adjusted to increase or decrease specificity when needed. PCR products were visualised with 1.5% agarose gel electrophoresis, purified with EXOSAP-IT (Affymetrix, Santa Clara, California, USA) and sequenced with the BigDye Terminator v3.1 Cycle Sequencing Kit (Applied Biosystems, Foster City, California, USA). Sequencing reactions were purified using ethanol precipitation and then analysed with an ABI 3130 Genetic Analyzer. Each of the 3′ to 5′ sequences was reverse-complemented and aligned with the corresponding 5′ to 3′ sequences and contiguous internal sequences using the program Geneious™ v7.1 (Drummond *et al.*, 2012), with the final sequence recovered from this consensus. The same software suite was used to perform multiple sequence alignment using the MUSCLE (Edgar, 2004) plug-in and to visualise the protein-coding sequences to confirm the amino acid reading frame, and check for stop codons.

TABLE 1. Gene lengths in base pairs, number of informative sites, percentage of informative sites, and appropriate model of evolution from MrModelTest.

Locus	Length (bp)	Informative sites	% Informative	Model used
16S	581	147	25.3	GTR + I + Γ
12S	459	107	23.3	HKY + I + Γ
ND2	1025	577	56.3	GTR + I + Γ
R35	710	73	10.3	HKY + I
NKTR	1113	120	10.9	GTR + I + Γ
PRLR	532	87	16.4	HKY + Γ
KIF24	572	86	15.0	GTR + I + Γ
MYH2	765	142	18.6	HKY + I
RAG1	1040	78	7.5	GTR + I + Γ
c-mos	407	30	7.4	HKY + I
BDNF	732	27	3.7	GTR + I
TOTAL	7936	1474	18.5	–

Phylogenetic analysis. We performed separate phylogenetic analyses with three commonly employed optimality criteria: Maximum Parsimony (MP), Maximum Likelihood (ML) and Bayesian Inference (BI). Analyses were performed on both the concatenated dataset and the individual genes. Parsimony analyses were run using PAUP* (Swofford, 2002) under the following conditions: 10 random addition replicates, tree bisection-reconnection (TBR) branch-swapping, zero-length branches collapsed to yield polytomies, and gaps treated as missing data.

For the ML and BI analyses the dataset was partitioned by gene, with the most appropriate model of evolution for each locus identified using Akaike information criterion in MrModeltest v2.3 (Nylander, 2008). Maximum Likelihood analyses were performed using Garli v2.0 (Zwickl, 2006). Phylogenetic robustness was estimated in the MP and ML analyses by running 1000 random addition bootstrap replicates (Felsenstein, 1985). The Bayesian analyses were conducted using MrBayes 3.2 (Huelsenbeck and Ronquist, 2003). Two separate Markov chains were run for 10 million generations, sampled every 1000 generations. If adequate convergence had not occurred after 5 million generations, additional generations were added until the average standard deviation of split frequencies was less than 0.01. Tracer v1.5 (http://tree.bio.ed.ac.uk/software/tracer) was used to plot the log likelihood score against generation to identify the convergence point, and the burn-in was discarded. Nodes that returned clade posteriors above 0.95 were considered significantly supported.

Morphological methods. We collected a series of 27 meristic and 15 mensural measurements from 73 alcohol-preserved specimens of Angolan and Namibian *Cordylus,* using dissecting microscopes and digital

calipers. Osteological data were obtained from nine specimens from the low-elevation area, four *C. machadoi* from near the type locality, and one *Cordylus* from the Vernay expedition, using High Resolution X-ray Computed Tomography (HRCT). These specimens were scanned using a Phoenix v|tome|x s CT scanner at the GE Inspection Technologies, LP Technical Solutions Center in San Carlos, California. Current, voltage, and detector-time were modified to optimise the grayscale range, and specimens were scanned in sections to maximise resolution (Table S2). Raw data were processed using GE's proprietary datos|x software v 2.3 to produce a series of tomogram images, which were then viewed, sectioned, measured and analysed using VG Studio Max 2.2 (Volume Graphics, Heidelberg, Germany). The skeleton and osteoderms were reconstructed separately for each scan to facilitate osteological analysis. The volume of the postcranial skeleton and osteoderms along the dorsal, ventral, caudal and limb areas were recorded for each of these scans.

For external morphology we followed the procedures of Greenbaum *et al.,* (2012) and Broadley and Branch (2002). We recorded morphometric data from preserved specimens, using digital calipers (0.01 mm) under a stereo-microscope. Measurements were taken on the right side of each specimen (on the left side if damaged): snout–vent length (SVL, tip of snout to anterior margin of vent); tail length (TL, posterior margin of vent to tail tip, measured only on specimens with complete and original tails); head length (HL, tip of snout to posterior margin of temporals); maximum head width (HW, measured at the broadest part); head height (HH, measured at midpoint of eye from top of head to bottom of lower jaw; snout–eye length (SEL, tip of snout to anterior margin of eye); snout–arm length (SAL, tip of snout to anterior margin of forelimb); axilla-groin distance (AGD, posterior edge of forelimb insertion to anterior edge of hind limb insertion); humerus length (HML); radius-ulna length (RUL); femur length (FL); tibia-fibula length (TFL); longest toe length (LTL, length of fourth toe on hind limb).

Scale counts (meristic data) were performed on the right side of each lizard (on the left side if damaged), except for femoral pore and generation gland counts if field/museum tags obscured the right thigh. Counts included: femoral pores (FP); generation glands (GEN); chin shields (CS); supralabials (SL, all scales bordering upper lip, except rostral, to posterior border of eye); infralabials (IL, all scales bordering lower lip, except mental, to large posterior labial [included]); supraoculars (SO); supraciliaries (SC); loreals (LO); suboculars (SOC, all scales bordering eye and in contact with the SLs with the exception of the anterior one [i.e. preocular]); preoculars (PRE); transverse row of gulars between posterior chin shields,(TGU, excluding small granular scales on either side); dorsal transverse rows (DTR, from immediately behind occipital to base of tail above vent); dorsolateral longitudinal rows (DLLR, midway between fore- and hind limbs, excluding small scales in the lateral fold); ventral transverse rows (VTR, axilla–groin); ventral longitudinal rows (VLR, midway between fore- and hind limbs, excluding small, often keeled, pseudo-ventrals on either side); caudal scales (CDS, counted around the tail at the position of the 11th and 15th scale to avoid possible differences between males [swollen tail base] and females); subdigital lamellae on fingers (SDF1 to SDF5) and toes (SDT1 to SDT5). Principal component analysis was performed on 10 mensural characters (standardized by SVL) and 22 meristic characters, using the prcomp command in R {stats}. Invariant characters were excluded from the PCA analysis and all remaining variables were scaled to have unit variance.

Results

The aligned, concatenated dataset contains 7921 characters, with 615 autapomorphies and 922 parsimony-informative characters. All phylogenetic analyses recovered the Angolan specimens as monophyletic, forming the earliest diverging lineage of the northern *Cordylus* clade (Fig. 3). Within this clade specimens of *C. machadoi* and the low-elevation specimens are strongly supported as being reciprocally monophyletic, with a genetic distance of 6.4–7.3% (average = 7.1%) for the mitochondrial marker ND2. The lowland forms display a degree of internal structure, with specimens from Iona (PEM R18005) and Pico Azevedo (CAS 254754, 254755, 256530, 256531) more closely related than the two specimens collected from Caraculo (CAS 254912, 256529). The specimens from the escarpment also show a degree of genetic diversity; the individual from Nasecute do Tchiviuguira (PEM R18009) is sister to a clade containing the specimens from the environs of Humpata (PEM R18006–8, 19782, 19784, KTH 09059).

Mensural and meristic data for the *C. machadoi* complex are summarised in Table 2. Lowland forms differ from *C. machadoi* and other east African *Cordylus* in several consistent characters, described in detail below and illustrated in Fig. 4. The HRCT data reveal a clear difference in osteodermal armament between high and low elevation forms: all *C. machadoi* lack osteoderms on the throat and venter, while adult specimens from lower

TABLE 2a. Variation in continuous measurements (mean and range) for specimens of *Cordylus namakuiyus* **sp. nov.**, *C. machadoi*, *C.* cf. *namakuiyus* (AMNH R47274–47321), and *C.* cf. *machadoi* from northern Namibia (TM 57561). All measurements following snout–vent length (SVL) are size-corrected (represented as percentage of SVL).

	Cordylus namakuiyus **sp. nov.**			*Cordylus machadoi*			*Cordylus* AMNH			Namibian *Cordylus*
	female	male	juvenile	female	male	juvenile	female	male	juvenile	juvenile
Number of specimens	5	1	4	5	4	5	22	16	10	1
SVL (mm)	92.20 (81.83–101.09)	89.67	52.52 (48.02–57.06)	89.26 (71.83–97.76)	85.10 (71.65–94.18)	57.04 (48.42–66.70)	90.39 (80.19–98.42)	86.93 (79.78–96.70)	74.35 (68.2–79.63)	43.9
Head length	26.69 (25.43–27.58)	27.26	30.51 (29.76–31.18)	27.93 (27.11–29.00)	28.91 (27.93–30.08)	29.84 (27.82–32.68)	29.06 (26.11–32.04)	30.86 (28.19–33.47)	30.24 (29.07–32.03)	32.71
Head width	23.45 (22.62–24.94)	25.34	22.71 (21.33–23.85)	23.17 (22.20–24.91)	23.82 (22.88–24.66)	22.51 (21.84–23.72)	24.32 (22.44–26.04)	25.70 (23.37–27.49)	24.91 (24.04–26.37)	22.3
Head height	11.56 (10.03–13.50)	12.23	12.03 (11.44–12.60)	10.33 (9.83–11.39)	10.82 (9.03–12.77)	11.65 (11.30 - 12.29)	11.22 (10.16–13.63)	11.56 (9.92–12.70)	11.31 (10.34–12.38)	11.87
Snout–Eye Length	9.29 (8.31–9.70)	9.65	11.39 (11.14–11.51)	9.81 (9.28–10.41)	10.13 (9.82–10.87)	10.54 (10.08 - 11.41)	9.91 (8.60–11.16)	10.01 (9.42–10.75)	9.96 (9.09–10.71)	12.23
Snout–Arm Length	38.55 (36.42–41.09)	39.48	43.14 (42.27–44.00)	39.20 (36.71–41.49)	40.34 (38.35–41.62)	42.67 (38.98 - 45.95)	39.31 (36.91–44.53)	40.97 (37.59–44.08)	41.44 (36.77–43.86)	45.85
Axila–Groin Distance	47.66 (43.85–51.42)	46.04	42.41 (37.82–45.19)	45.98 (43.84–49.27)	43.94 (42.07–45.71)	41.05 (38.38 - 44.18)	45.72 (41.62–49.26)	44.67 (41.84–47.67)	44.51 (42.29–48.25)	36.79
Humerus ML	13.28 (12.34–14.44)	13.69	14.25 (12.99–15.04)	12.51 (10.45–14.30)	12.64 (12.41–12.85)	13.31 (10.44 - 17.10)	13.97 (13.10–15.58)	14.05 (11.87–15.65)	13.95 (13.10–15.25)	12.82
Radius–Ulna length	12.22 (11.38–13.12)	11.92	12.81 (12.50–13.46)	11.34 (10.55–12.03)	12.24 (11.47–12.92)	11.31 (9.99 - 12.14	12.02 (10.96–14.21)	12.08 (10.72–13.32)	12.32 (11.41–13.15)	12.35
Femur length	18.76 (17.85–19.26)	18.27	19.46 (18.07–20.36)	18.28 (16.93–19.30)	19.00 (17.15–20.44)	17.99 (16.59 - 19.19)	19.18 (17.24–21.10)	20.08 (19.00–21.12)	19.92 (18.93–21.03)	17.81
Tibia–fibular length	15.24 (13.85–16.23)	15.48	15.62 (13.46–17.35)	13.79 (13.36–14.80)	14.66 (11.95–16.34)	14.81 (12.72 - 17.03)	15.24 (13.50–16.66)	15.79 (14.80–17.48)	15.46 (14.74–16.12)	14.58
Longest toe length	10.84 (9.91–11.45)	10.15	15.05 (13.25–16.89)	12.22 (11.11–12.82)	11.78 (11.25–12.11)	14.15 (12.54 - 16.49)	12.62 (11.52–13.82)	13.07 (11.77–14.23)	13.85 (13.00–15.15	13.17

TABLE 2b. Meristic and qualitative variation (median and range) for specimens of *Cordylus namakuiyus* **sp. nov.**, *C. machadoi*, *C.* cf. *namakuiyus* (AMNH R47274–47321), and *C.* cf. *machadoi* from northern Namibia (TM 57561).

	Cordylus namakuiyus **sp. nov.**			*Cordylus machadoi*			*Cordylus* AMNH			Namibian *Cordylus*
	female	male	juvenile	female	male	juvenile	female	male	juvenile	juvenile
Number of specimens	5	1	4	5	4	5	22	16	10	1
Chin shields	5 (5–6)	5	5	5	5	5	5	5	5 (5–6)	5
Femoral pores	5 (4–6)	5	0 (0–6)	6 (6–7)	6 (5–7)	6 (5–6)	5 (4–6)	5 (4–6)	5 (4–6)	5–6
Generation glands	0	12	0	0	18 (12–22)	0–16	0	13 (11–15)	0	0
Supralabials	5 (4–5)	5	5	5	5	5	5 (5–6)	5 (4–6)	5 (5–6)	5
Infralabials	5 (5–6)	5	5	6 (5–6)	6 (5–6)	5	5 (4–6)	5 (4–6)	5 (4–5)	6
Supraoculars	4	4	4	4	4	4	4	4	4	4
Supraciliaries	3	3	3	3	3	3–4	3	3	3	3
Loreal	1 (0–1)	1	1	1	1	1	1	1	1	1
Suboculars	3 (2–3)	3	3	3 (3–4)	3	3	3 (3–4)	3 (3–4)	3	3
Preoculars	1	1	1	1	1	1	1	1	1	1
Transverse gular scales	15 (14–17)	15	16 (15–16)	22 (17–21)	19 (18–20)	18 (18–24)	17 (15–18)	17 (15–18)	17 (16–18)	20
Dorsal transverse rows	25 (24–26)	24	23.5 (23–25)	25 (24–28)	24.5 (23–26)	25.5 (25–28)	24 (23–25)	24 (22–24)	24 (23–25)	24
Dorsolateral longitudinal rows	24	23	24 (23–24)	26 (22–27)	23	23.5 (23–24)	23 (22–25)	23 (20–24)	22 (20–24)	22
Ventral transverse rows	22 (21–24)	22	21.5 (21–22)	23 (21–25)	21.5 (21–26)	21 (20–22)	22 (20–23)	22 (21–23)	22 (21–23)	23
Ventral longitudinal rows	16 (15–16)	17	15.5 (14–16)	16 (14–18)	16 (13–16)	13.5 (13–14)	14 (13–16)	14 (12–15)	13 (12–14)	14

TABLE 2c. Meristic variation (continued) for specimens of *Cordylus namakuiyus* **sp. nov.**, *C. machadoi*, *C.* cf. *namakuiyus* (AMNH R47274–47321), and *C.* cf. *machadoi* from northern Namibia (TM 57561).

	Cordylus namakuiyus **sp. nov.**			*Cordylus machadoi*			*Cordylus* AMNH			Namibian *Cordylus*
	female	male	juvenile	female	male	juvenile	female	male	juvenile	juvenile
Number of specimens	5	1	4	5	4	5	22	16	10	1
Caudal scales 11th whorl	11 (10–12)	10	10	10.5 (10–11)	10	10	11 (9–12)	10 (9–12)	10 (8–11)	11
Caudal scales 15th whorl	10 (9–10)	10	10	9 (8–10)	10.5 (10–11)	9	10	–	–	–
Subdigital lamellae F1	5 (5–6)	6	6 (5–6)	5	5 (4–6)	5 (5–6)	5 (5–6)	5 (5–6)	5 (5–6)	5
Subdigital lamellae F2	8 (7–9)	8	9 (9–10)	8 (8–9)	8 (7–9)	8 (8–9)	8 (7–9)	8 (7–9)	8 (8–9)	8
Subdigital lamellae F3	11 (10–12)	11	11 (11–12)	11 (11–12)	11 (9–11)	11	11 (10–12)	11 (10–12)	11 (10–11)	11
Subdigital lamellae F4	12 (11–13)	12	13 (12–13)	11 (11–13)	11 (9–11)	11	12 (10–14)	12 (11–13)	12 (11–13)	10
Subdigital lamellae F5	8 (7–9)	8	9 (8–9)	8 (8–9)	8 (7–9)	8	8 (6–9)	8 (6–9)	8 (7–9)	8
Subdigital lamellae T1	6 (5–7)	6	6 (5–7)	6	5	6	6 (5–9)	6 (5–6)	6	5
Subdigital lamellae T2	9 (8–10)	9	9.5 (8–10)	10 (8–10)	8 (8–9)	9.5 (9–10)	9 (8–14)	9 (8–10)	9 (8–10)	7
Subdigital lamellae T3	12 (11–12)	11	12 (11–14)	12 (12–13)	12 (10–12)	12 (11–12)	12 (11–13)	11 (11–14)	12 (11–14)	11
Subdigital lamellae T4	14 (13–14)	13	15 (14–17)	14 (12–15)	13 (11–14)	14	13 (10–14)	13.5 (12–15)	14 (13–15)	13
Subdigital lamellae T5	10 (10–11)	11	10.5 (10–12)	11 (10–12)	10 (9–11)	10 (10–11)	10 (7–11)	10 (9–11)	10 (9–11)	10

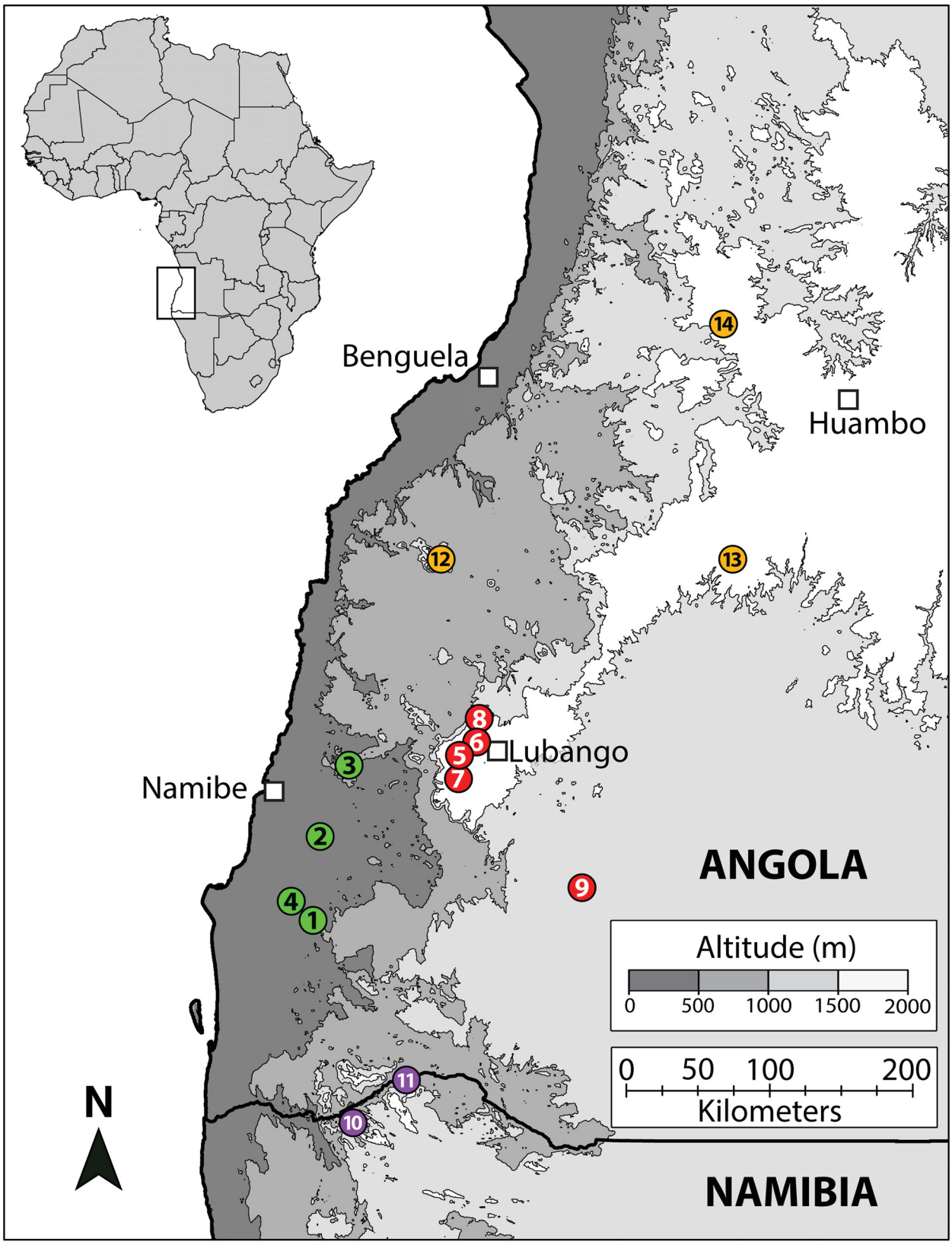

FIGURE 2. Map showing localities for *Cordylus* in Angola and Namibia. *Cordylus namakuiyus* **sp. nov. 1)** Iona national park: PEM R18005, **2)** Pico Azevedo: CAS 254754, 254755, 256529–31, **3)** Caraculo: CAS 254912, 256529, **4)** Iona National Park: TM 40430. *C. machadoi*: **5)** Humpata environs: PEM R18006–8, 19782, 19784, **6)** Nasecute do Tchiviuguira: PEM R18009, **7)** NMN 7002, **8)** TM 40131–3, **9)** TM 40095, 40096. *C.* cf. *machadoi*: **10)** Otjihipa Mountains: NCN–FN 377, 378, **11)** Baynes Mountains: TM 57561, NCN-FP 402, 403, **12)** Sera de Neve (sight record, P. Vaz Pinto), **13)** *C. angolensis*, Caconda: type locality, and **14)** Mombolo: AMNH 47331–35.

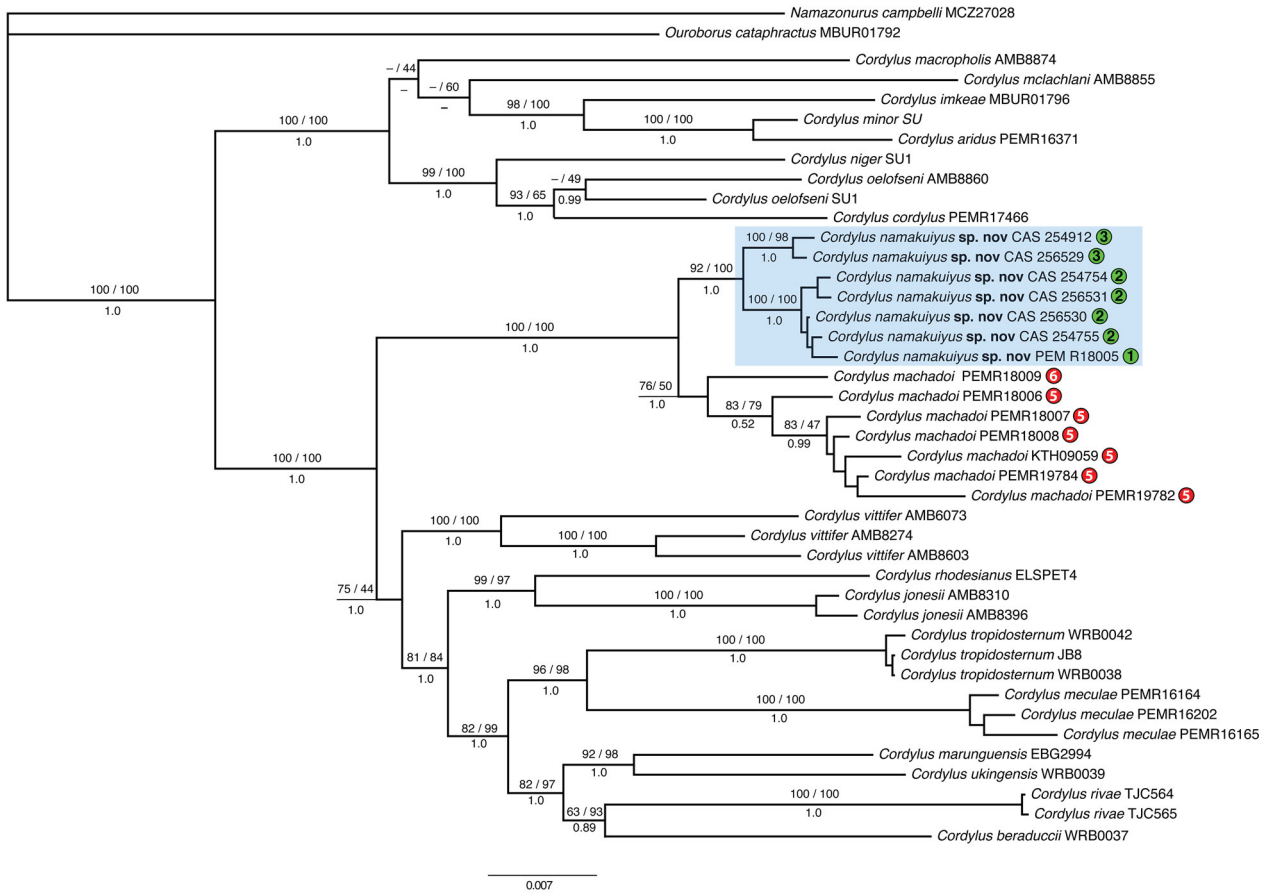

FIGURE 3. Maximum likelihood phylogeny of 11-gene dataset of *Cordylus*. Bootstrap support for MP and ML shown above branches, Bayesian posterior probabilities below. The new species, *Cordylus namakuiyus* **sp. nov.**, is highlighted for reference. The numbered circles to the right of the Angolan specimens correspond to the numbered localities in Figure 2.

elevations, and the AMNH specimen, possessed a significant amount of ossified ventral armor (Fig. 5). Significant ontogenetic variation in the degree and arrangement of osteoderm armour was seen in both high- and low-elevation *Cordylus* (see Supplementary Fig. S3). In low-elevation specimens late-stage fetuses (CAS 254913, 254914, SVL = 48.0–48.6 mm) lack body osteoderms entirely; one juvenile (CAS 256529, SVL = 56.5 mm) displays attenuate osteoderms restricted to the tail, limbs and lateral aspects of the dorsum; a slightly larger juvenile (CAS 256530, SVL = 57.0 mm) has well-developed osteoderms covering its dorsum, limbs and tail; while adults (CAS 254912, 256531, PEM R18005) and subadults (CAS 254754, 254755) are entirely covered in thick imbricated osteoderms, save for the axillary and inguinal areas and around the cloaca. The *C. machadoi* specimens also exhibit an increase in armour across their ontogenetic series, although they are consistently less well armoured than their lowland equivalents at each stage of development (Table 3). Two low-elevation specimens, CAS 254912 and PEM R18005, have regenerated tails with osteoderms that are indistinguishable from those of original tails, while two others CAS 256530 and CAS 256531, have actively regenerating tails that lack osteoderms entirely. The principal component analyses of the mensural-meristic and meristic-only datasets explain 33% and 34% of the variation in the first two principal components, respectively (See supplementary table S4 for loadings). Both the combined and meristic-only datasets recovered *C. machadoi* and the low-elevation specimens as forming two distinct clusters in the first two principal components of morphospace. The AMNH specimens clustered with adult specimens of the low-elevation form in both PCAs, and resemble the lowland form in a number of pholidosic characters. The single juvenile specimen from Namibia (TM 57561) clusters with the high-elevation form in both PCAs (Fig. 6).

TABLE 3. Volumetric measurements of postcranial skeleton and osteoderms for CT-scanned specimens of *Cordylus*. § denotes a juvenile or neonate, * marks an autotomised tail that is missing or partially regenerated.

Accession number	Species	Postcranial skeleton	Dorsal osteoderm	Caudal osteoderm	Ventral osteoderm vol.	Limb osteoderm vol.
CAS 254912	*C. namakuiyus* **sp. nov**.	830.57	717.46	792.74	267.22	490.98
CAS 254913	*C. namakuiyus* **sp. nov.**§	129.17	0	0	0	0
CAS 254914	*C. namakuiyus* **sp. nov.**§	125.15	0	0	0	0
CAS 254754	*C. namakuiyus* **sp. nov.**	522.09	356.21	515.80	102.65	214.82
CAS 254755	*C. namakuiyus* **sp. nov.**	649.26	519.96	810.17	274.45	411.15
CAS 256529	*C. namakuiyus* **sp. nov.**§	112.62	10.61	39.33	0	12.24
CAS 256530	*C. namakuiyus* **sp. nov.**§	167.21	101.45	145.35*	16.21	80.38
CAS 256531	*C. namakuiyus* **sp. nov.**	862.79	686.85	737.33*	365.83	463.54
PEM R18005	*C. namakuiyus* **sp. nov.**	815.90	736.66	1061.13	352.06	498.57
AMNH 47301	*C. cf. namakuiyus* **sp. nov.**	958.56	654.51	702.76	211.29	387.83
PEM R18006	*C. machadoi*	581.26	298.63	630.65	0	169.02
PEM R18009	*C. machadoi* §	112.94	2.14	70.76	0	8.87
PEM R19782	*C. machadoi*	610.13	322.59	412.59*	7.33	201.99
PEM R19784	*C. machadoi*	598.03	300.28	343.24	1.89	188.68

Taxonomic account

***Cordylus namakuiyus* sp. nov.**
(Figs. 1–6, Table 2)

Holotype. CAS 254912, an adult female collected from a large rock outcrop near Caraculo, on the road from Lubango and Namibe, Namibe province, Angola [15°0'59.40"S, 12°38'31.30"E; 503 m elevation], collected by E. L. Stanley, S. de Sá, S. Bandeira, H. Valerio, A. L. Kuhn, J. V. Vindum and L. Ceríaco, on 6 December 2013.

Paratypes. Eight specimens: CAS 254913–14, two fetuses taken from the holotype, with the same data; CAS 256529, one juvenile collected at the same locality as the holotype [15°0'57.3"S, 12°38'32.6"E; 509 m elevation] by the same collectors; CAS 254754, adult female, CAS 254755, adult male, CAS 256530, juvenile, CAS 256531, adult female, all collected on the outskirts of Pico Azevedo [15°28'33.2"S, 12°27'45.7"E; 421 m elevation] by the same collectors of the holotype on 7 December 2013; PEM R18005, adult female, collected in a low rock outcrop bordering the road between Namibe and Omahua lodge [15°59'48.5"S, 12°24'24.6"E; 308 m elevation], Namibe Province, Angola, by W. R. Branch, K. A. Tolley and G. J. Measey on 20 January 2009.

Additional material. Forty-nine specimens. One specimen: TM 40430, adult female from 49 km ESE of Tombua, Namibe Province, Angola [15°53'S, 12°16'E], collected by W. D. Haacke on 31 March 1971; and a series of 48 specimens collected by A. S. Vernay, H. Lang and R. Boulton between 25 April and 4 August 1925, locality "Angola": Adult females: AMNH R47274, 47276, 47278, 47279, 47282–84, 47286, 47287, 47289-95, 47297, 47298, 47299, 47304, 47305, and 47315. Adult males: AMNH R47275, 47277, 47280, 47281, 47285, 47288, 47296, 47300–03, 47306–09, and 47311. Juveniles: AMNH R47310, 47312–14, and 47316–23.

Diagnosis. A relatively large species of *Cordylus*, identified to genus by the following combination of characters: four-limbed, rupicolous, viviparous, strongly depressed triangular head and body, osteoderms present, rhomboidal, imbricate and keeled dorsal scales present, occipitals non-spinose, and spinose caudal and limb scales enlarged (Branch 1998; Broadley and Branch 2002; Stanley *et al.,* 2011). *Cordylus namakuiyus* **sp. nov.** differs from all other species in the genus except for *C. vittifer* and *C. machadoi*, by the presence of a transverse row of elongated dorsal scales immediately posterior to occipitals (vs. absence); from *C. vittifer* by possessing an incomplete row of pre-occipital scales between posterior parietal and occipital scales (absent in *C. vittifer*), and by having infralabials that are moderately-deeply corrugated (vs. usually smooth); from *C. machadoi* by having a large, keyhole-shaped interparietal in broad contact with frontoparietals, thereby separating anterior parietals (vs. small, diamond-shaped interparietal not in contact with frontoparietal, thereby never completely separating anterior parietals), temporal scales that are strongly keeled (vs. weakly keeled), fewer transverse gular rows (14–17 vs. 17–24), light brown dorsal body coloration (vs. darker brown), and by the absence of dark speckles on throat and ventral body surfaces (vs. presence), presence of osteoderms on throat and ventral surfaces (vs. absence); from *C. angolensis* (based on original description; Bocage 1895) by having fewer ventral transverse scale rows (21–24 vs. 27), light brown dorsal body coloration (vs. brown with blackish speckles over paler dorsal ground coloration), and by the absence of longitudinal series of whitish speckles along dorsal surface (vs. presence of two longitudinal series of small whitish speckles along dorsum), and presence of a loreal (vs. absence).

Description of holotype. SVL 101 mm. Head and body depressed. Head 1.2 × as long as broad. Nasals in median broad contact; frontonasal lozenge-shaped, as broad as long, separated from frontal by enlarged prefrontals (in median contact, forming a suture), separated from rostral by nasals, separated from loreal by prefrontals; frontal in contact with first and second supraoculars, followed by a pair of large frontoparietals in broad, median contact; a distinctive keyhole-shaped interparietal in broad contact with the frontoparietals, separating anterior parietals; parietal eye visible; a row of 10 rugose occipitals. A row of 11 elongated nuchal scales. Four supraoculars and three supraciliaries. Nasals large, with nostril pierced centrally on upper margin. Loreal in contact with preocular, nasal and first two supralabials; three suboculars, well separated from the lip by the fourth and fifth supralabials. Rostral twice as broad as deep; supralabials five; infralabials five; chin shields five. Mental twice as broad as long; gulars smooth, enlarged and forming transverse rows posteriorly, with 16 gulars between the posterior extent of the jaws. Dorsal scales rectangular, rugose, obtusely keeled, mucronate and serrate posteriorly; dorsals and laterals in 25 transverse and 24 longitudinal rows; ventrals squarish, smooth, in 21 transverse and 15 longitudinal rows. Scales on limbs above large, strongly keeled and spinose; subdigital lamellae under fourth toe 14; femoral pores five; generation glands absent. Tail with whorls of large, elongate, strongly keeled, spinose and serrated scales, spines directed posteriorly and largest superolaterally.

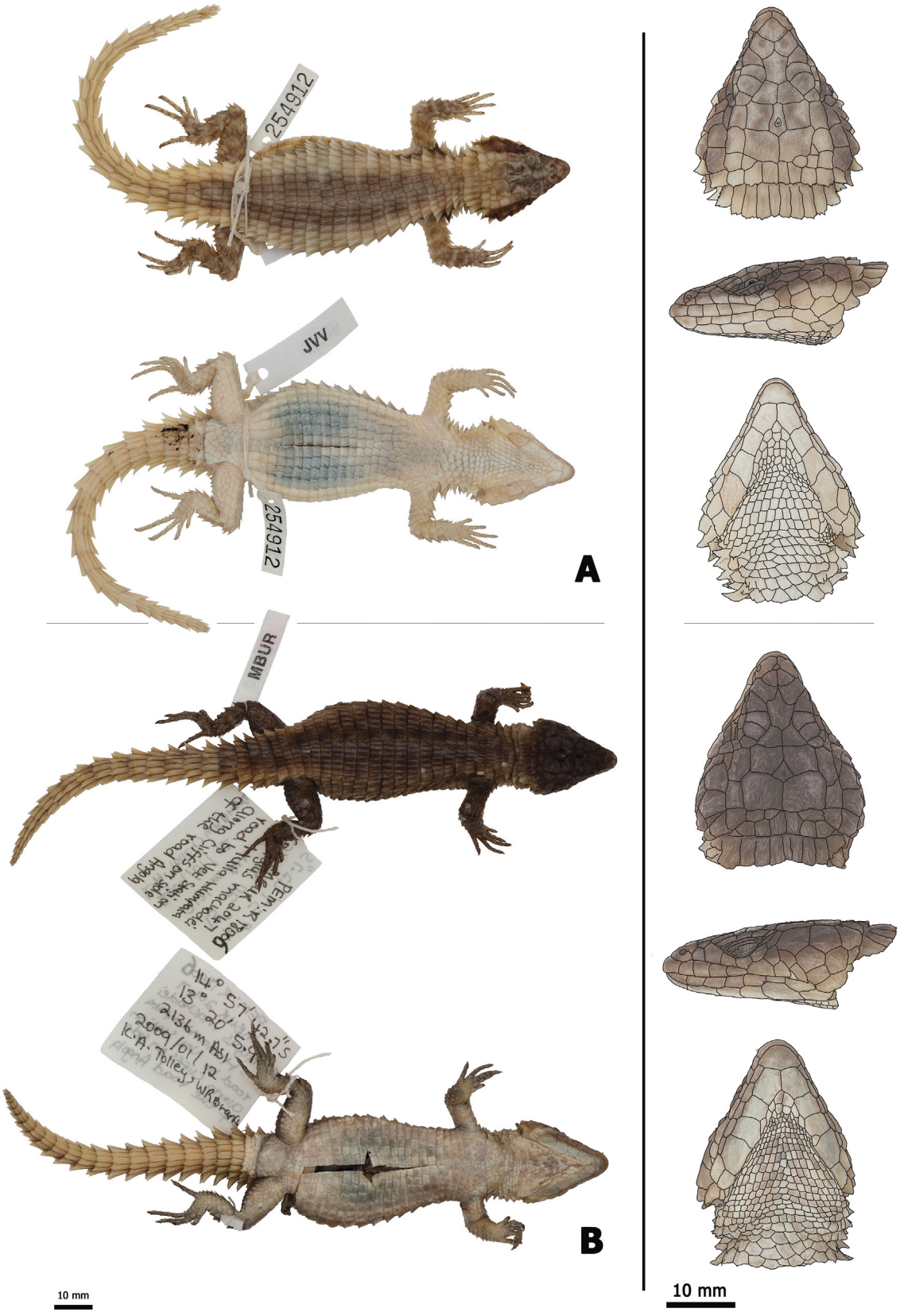

FIGURE 4. Dorsal, lateral, and ventral views of **A)** *Cordylus namakuiyus* **sp. nov.** (CAS 254912, holotype) and **B)** *C. machadoi* (PEM R18006).

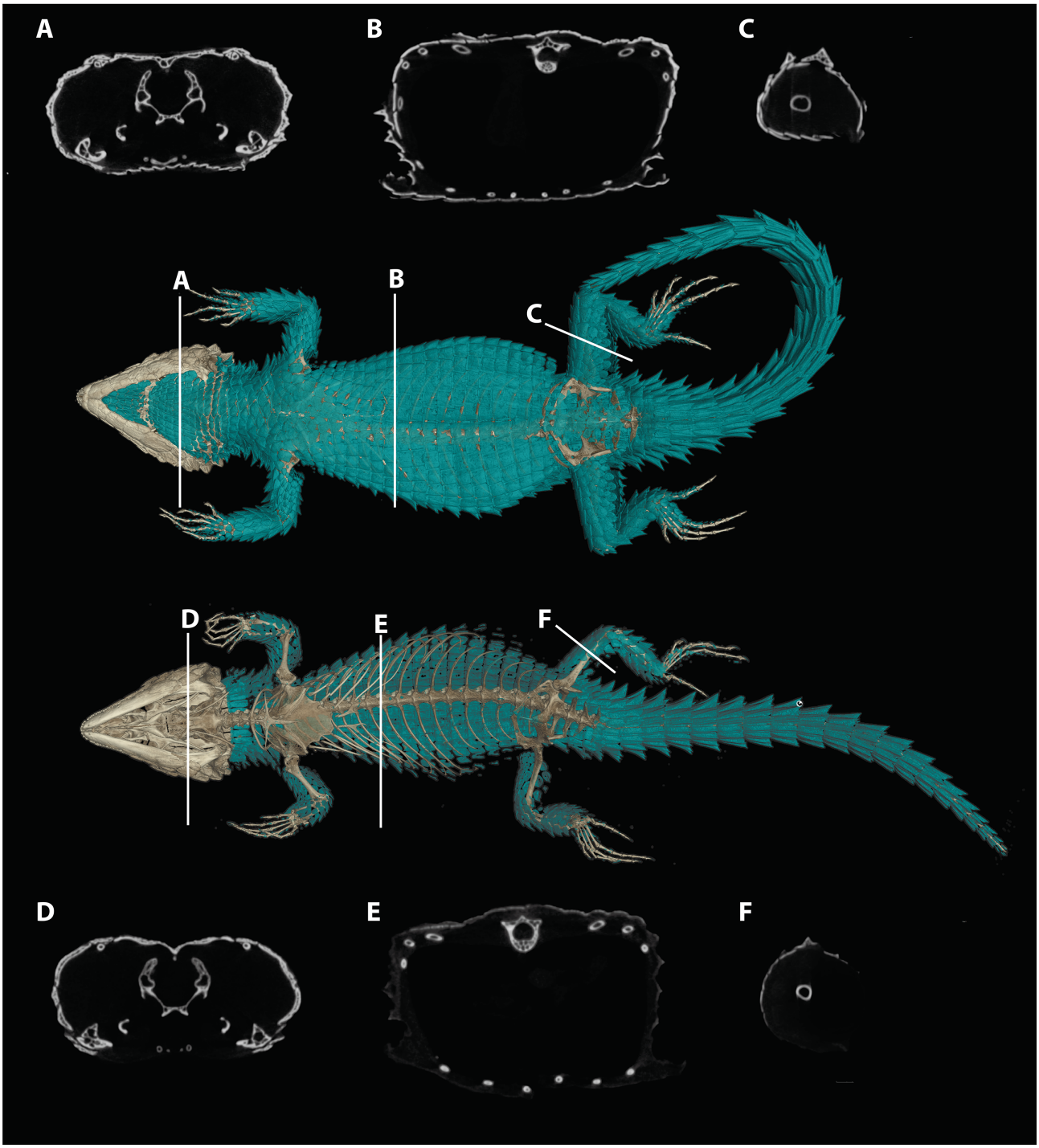

FIGURE 5. High-resolution Computed Tomography reconstructions showing the ventral aspects of (top) *Cordylus namakuiyus* **sp. nov.** (CAS 254912, holotype) and (bottom) *C. machadoi* PEM R18006. Osteoderms are shown in green. A–F tomograms showing cross-sections of the throat (A+D), torso (B+E), and hind limb (C+F).

Cranial osteology. The parietal is pentagonal with a well-developed, unbifurcated medio-posterior process that extends past the postero-lateral processes. The premaxilla is unpaired and contains seven pleurodont teeth and five foramina, with a dorsal process that extends posteriorly to be clasped by the nasals, which themselves insert into an unpaired frontal. The maxilla is typically scinciform, with a deeply grooved crista dentalis and 16 pleurodont teeth. No palpebral is present, though the prefrontal has a small, flattened, laterally projecting tubercle that supports the anterior-most superorbital osteoderm in much the same way. The jugal is triangular in cross-section and asymmetrically T-shaped, with a tapering anterior process and a broad, truncated posterior process that extends along and past the posterior edge of the maxilla. The lacrimal bone is small, flattened and extends along the

postero-ventral boundary of the maxilla and prefrontal. Edentate pterygoids extend back to connect with the quadrates, becoming C-shaped in cross-section posterior to the epipterygoid condyle. The squamosal is curved and blade-like, circular in cross-section anteriorly, becoming flattened posteriorly, where it articulates with the cephalic condyle of the quadrate and the braincase. Supratemporals are flattened, reniform and fused to the paroccipital processes. The supraoccipital has a strong sagittal crest that extends posteriorly to contact the ventral surface of the medio-posterior process of the parietal. The prootic bears an extended alar process and a well-developed, rhomboid christa prootica, and a very weak supratrigeminal process. Basipterygoid processes are well developed and flattened. The lower jaw possesses a large adductor fossa, a highly flattened and medially extended retroarticular process, a medially open meckelian canal and a dentary with a strong subdental shelf, 21 mandibular teeth, and nine dentary foramina.

Postcranial osteology. The holotype possesses 25 presacral and 17 postsacral vertebrae with the last 21 mm (roughly 20%) of the tail made up of regenerated cartilage. There are five cervical ribs, three sternal ribs, two xiphisternal ribs, five long asternal ribs with ossified costal cartilage, and eight short asternal ribs. The first three cervical ribs are distally flattened with bifid cartilaginous projections. Sacral vertebrae are fused asymmetrically, with the left diapophysis formed from the fused sacral ribs, while the right diapophysis is formed by the fusing of the second sacral and first caudal ribs. The next two pairs of caudal ribs are well developed and angled anteriorly, with subsequent ribs becoming increasingly smaller and posteriorly angled. Pelvic girdle is well developed and flattened. No iliac tubercle is present. There is a well-developed, ventrally angled pubic tubercle directly anterior to the obturator foramen. Both hypoischium and hyperischium are well developed. Pubic bones are well separated by triangular prepubic cartilage. The sternal plate is broad and lacks a fontanelle. Interclavicle cruciform, clavicles rod-like and flattened dorsally. The epicoracoid is narrow and curved, connecting the scapular ray to the primary and secondary coracoid rays, but not to the anterior process of the scapular. Limb bones well developed. Digits display the typical squamate phalangeal arrangement of 3–5–4–3–2. A large sesamoid is found in the palm of the hands. The fifth metatarsal possesses an elongated medial process at midbody.

Osteoderms. Scales of the dorsal and temporal regions of the skull and the ventrolateral aspects of the jaws are underlain with rugose osteoderms. These osteoderms fuse to the proximal parietal, frontal and postorbital bones, although the mesokinetic and metakinetic joints appear unobstructed and flexible. The entire body is covered in robust osteoderms, with only the femoral pores and the axillary, inguinal and cloacal regions unarmoured. Large, rectangular, imbricate osteoderms protect the dorsal and lateral aspect of the trunk, becoming more keeled and mucronate laterally. Unkeeled, imbricate osteoderms cover the entire venter, from the gulars to the cloaca, rectangular on the throat and abdomen, becoming rhomboid around the sternum and cloaca. Several abdominal osteoderms appear to be fractured. Caudal osteoderms are thick, sharply spined and arranged in imbricate transverse whorls. Limbs covered by imbricate circular/rhomboid osteoderms, keeled and mucronate dorsally, plate-like ventrally.

Colouration of holotype. Dorsal coloration is medially brown, blending to a straw-yellow laterally. Head yellow-brown; supra and infralabials yellowish; a dark-brown bar extends from the posterior aspect of the eye to the temporals. The base of the tail is medially brown, surrounded by a straw-yellow coloration that extends towards the tip and eventually dominates the tail; the dorsal aspect of the limbs is brown. Laterally a dark-brown line, similar to the eye-mask coloration, extends from the neck towards the insertion of the forelimbs. The venter is yellowish-white, cream on the tail; the underside of the hind limbs, cloacal region and tail are cream, grading into yellowish on the anterior half of the tail.

Variation. Variation in scalation and body measurements of *C. namakuiyus* **sp. nov.** are reported in Tables 2 and 3. The sole male paratype CAS 254755 has 12 generation glands on the ventral surface of each thigh. One female paratype (CAS 254754) differs from the holotype in having the loreal and preocular fused. The medioposterior parietal process is slightly bifurcated distally in CAS 254754, CAS 265529 and PEM R18005, and does not extend back beyond the posterolateral processes in CAS 25630. Five premaxillary foramina are present in all type specimens except CAS 254754 (two) and CAS 256531 (four). Specimens CAS 254755 and PEM R18005 have 15 maxillary teeth, and CAS 256531 has 17. All paratypes have 21 mandibular teeth, except CAS 254754 (20), CAS 256530 (18), and CAS 254755 and CAS 256529 (16). The supratemporals are not fused to the paroccipital processes in CAS 254754, CAS 256529, and CAS 256530. Five of the paratypes have full, un-autotomised tails: CAS 254755 has 29 postsacral vertebrae, CAS 25474, CAS 256529 each have 27, and the two fetuses, CAS 254913 and CAS 254914, have 25 and 26 respectively. One specimen, CAS 256531, has 26 presacral

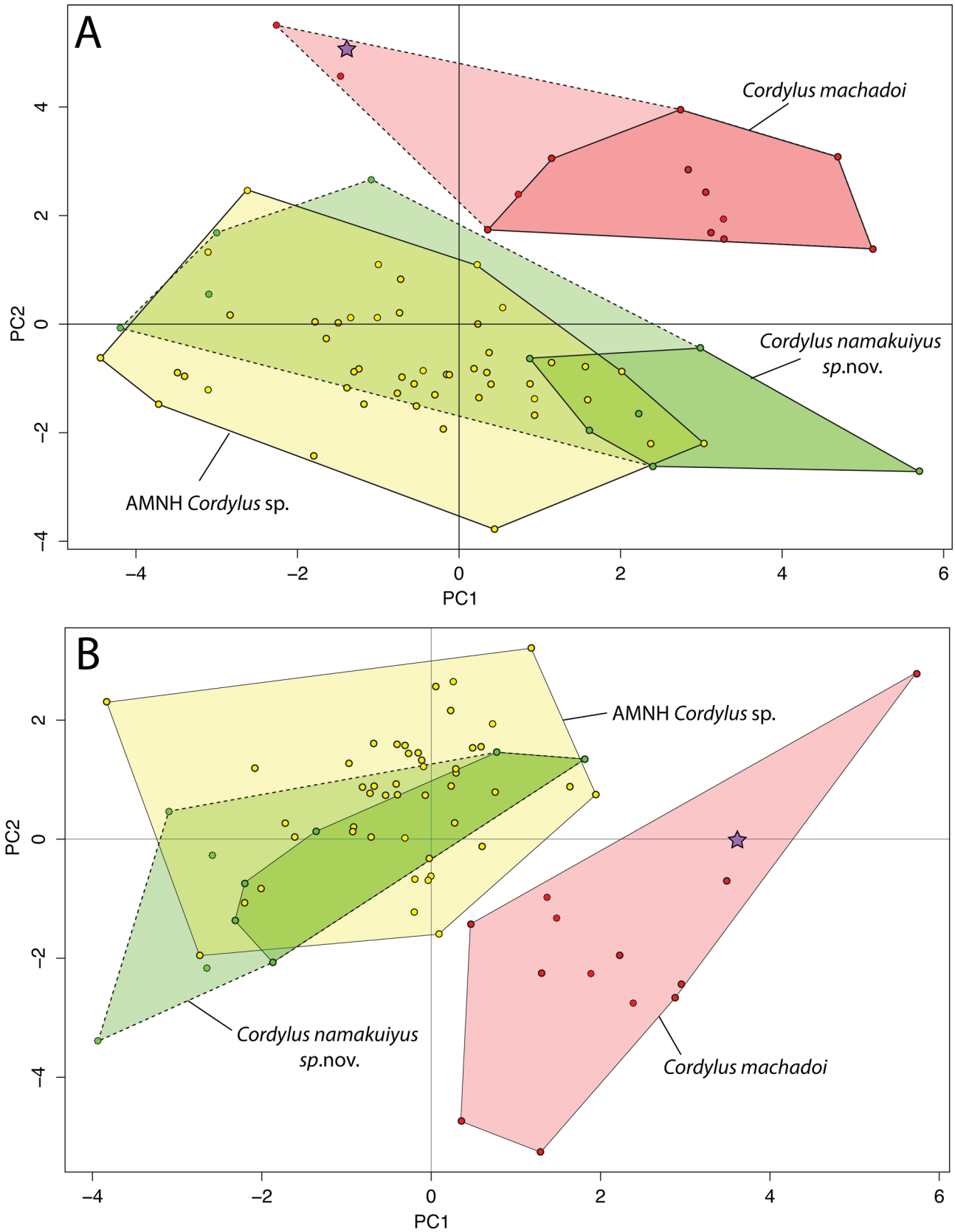

FIGURE 6. PCA plots of A) 32 meristic and continuous and B) 22 meristic characters from 73 specimens of *Cordylus*. Green dots = *C. namakuiyus* **sp. nov.** (N = 10), red dots = *C. machadoi* (N = 13), yellow dots = AMNH *C.* cf. *namakuiyus* collected on the 1925 Vernay expedition (N = 48), purple star = *C.* cf. *machadoi* (TM 57561) from northern Namibia. Polygons with solid lines show morphospace of adult specimens, those with dotted lines represent morphospace of adults + juveniles.

vertebrae. CAS 254755, CAS 256529 and CAS 256530 each possess four pairs of long asternal ribs, while CAS 256529 and PEM R18005 each have seven short asternal ribs. None of the paratypes exhibit the asymmetrical sacral fusion of the holotype, but rather display the normal condition of having the sacral diapophyses formed from the sacral ribs. The hyperischium of CAS 254755 extends anteriorly to connect with the prepubic cartilage.

Etymology. The specific epithet "*namakuiyus*" is the masculine latinised form of namakuiya, which means "thorny" in the Herero language, referring to the sharp spines on the limbs and tail of this species. Suggested common name: Kaokoveld Girdled Lizard.

Distribution. Currently, the new species is known only from the south and central parts of Namibe Province, Angola, southwest of the Leba escarpment, at elevations of 215–509 m a.s.l.

Localities. Angola: AMNH R47274–47321. Namibe Province, outskirts of Caraculo: CAS 254912–14 [15°0'59.4"S, 12°38'31.3"E; 503 m elevation], CAS 256529 [15°0'57.3"S, 12°38'32.6"E; 509 m elevation]; outskirts of Pico Azevedo: CAS 254754–55, 256530, 256531) [15°28'33.2"S, 12°27'45.7"E; 421 m elevation]; Road from Namibe to Omahua lodge PEM R18005 [15°59'48.5"S, 12°24'24.6"E; 308 m elevation]; 49 km ESE of Tombua: TM 40430 (15°53'S, 12°16'E; 215 m elevation).

Habitat and natural history notes. This species is found in gently sloping crevices of granite outcrops in the arid Kaokoveld. When approached, specimens retreat into their fissure as far as possible, wedging themselves head-first and protecting their head and flanks with their spiny tails. As with all other cordylines, *C. namakuiyus* **sp. nov.** is viviparous; the holotype contained two large fetuses (SVL 49.5% of the holotype). The fetuses appear to be approaching full-term, suggesting a spring/early summer parturition period. Although these fetuses lack any body osteoderms, the slightly larger neonates (SVL 55.6–56.4% of the holotype) possess significant dermal ossification, suggesting that the young rapidly accumulate osteodermal armour following parturition. One of the Pico Azevedo specimens was found occupying the same rock crack as an adult *Chondrodactylus pulitzerae* (Schmidt), and PEM R18005 from Iona National Park inhabited the same crack as an adult *Chondrodactylus fitzsimonsi* (Loveridge).

Discussion

The phylogenetic and morphological assessment of *Cordylus* from southwestern Angola provides multiple lines of evidence that the low-elevation form represents a species distinct from the escarpment-dwelling *C. machadoi.* The discovery of an undescribed *Cordylus* species from southwestern Angola—one of the better-explored areas of the country—underlines how little is known about the country's biodiversity. Angola contains roughly two-thirds the number of reptile species of South Africa, and less than one-fifth the number of endemic reptiles (www.reptile-database.org), despite occupying a similar land area and latitudinal range. This dichotomy is partly a result of the protracted Angolan independence and civil wars, which have significantly limited scientific collecting during the age of molecular systematics. As a result, Angolan taxonomy has not been as affected by the recent advances in molecular phylogenetic approaches that facilitate the identification of cryptic and/or recently diverged species. Scientific collecting has recently restarted, following the cessation of the civil war in 2002, and has resulted in the description of several new squamate species from southern Angola (Haacke, 2008; Conradie *et al.*, 2012). The fact that the range-restricted *C. machadoi* concealed a cryptic species suggests that its northern congener, *C. angolensis*, which has a comparatively broad geographic distribution, may itself represent a species complex. The taxonomic status of *C. angolensis* is the focus of ongoing work (Bates *et al.*, unpublished data).

The specimens of "*Cordylus cordylus"* collected during the AMNH's 1925 Vernay expedition cluster closely with adult specimens of the lowland species in our principal component analysis, and agree with the new species in possessing an enlarged interparietal that separates the anterior parietals, having a dark band along the lateral aspects of the head, and possessing osteoderms on the throat and venter. Although the Vernay specimens lack specific locality information, the expedition field notes mention that significant numbers of unidentified lizards were collected at Pico Azevedo and 100 km east of Moçâmedes (presently Namibe city), the same areas where the eight CAS specimens of the new species were collected. We therefore feel confident in assigning the Vernay material to *C. namakuiyus* **sp. nov.** The identity of the juvenile specimen (TM 57561) from the Otjihepa Mountains in northern Namibia is less certain: its diamond-shaped interparietal, high elevation locality, and the results of the principal component analysis on the combined character dataset and meristic characters (Fig. 6), all suggest it

belongs to *C. machadoi*. However, the interparietal divides the anterior parietal, as seen in *C. namakuiyus* **sp. nov.**, and it is more geographically isolated from all other records of *C. namakuiyus* **sp. nov.** and *C. machadoi* than either species is from each other. Given this conflict, further sampling and analysis is warranted to ascertain the identity of the cordylids in this population.

Our phylogenetic analyses of *Cordylus* return a similar topology to those of the two most recent studies—Greenbaum *et al.* (2012) and Nielsen and Colston (2014)—while increasing support for the deep relationships. Within the northern *Cordylus* group Angolan species diverged earliest, followed by the southernmost species *C. vittifer*. These results differ from the phylogeny of Stanley *et al.* (2011) which placed *C. vittifer* as the earliest diverging lineage and recovered *C. machadoi* as sister to the Zimbabwe/Mozambique species *C. rhodesianus* (Hewitt). It is worth noting that, under this new arrangement, the two earliest diverging lineages within the northern *Cordylus* clade—*C. machadoi* + *C. namakuiyus* **sp. nov.** and *C. vittifer*—occur in the "Southern African" biogeographical region *sensu* Linder *et al.* (2012), while all other members of the northern *Cordylus* group occur in the "Zambezian" or "Somalian" biogeographical regions. As no other cordylines (except two species of *Smaug* Stanley and three species of *Chamaesaura* Schneider) occur outside the Southern African region, this suggests that *Cordylus* have shifted major biogeographical regions only twice, from the Southern African to Zambezian region following the split between *C. vittifer* and East African species, and from the Zambezian to Somalian region in the *C. beraduccii* Broadley and Branch + *C. rivae* (Boulenger) clade. No tissues from the central Angolan species were available for this study, and the phylogenetic placement of *C. angolensis* remains unknown. However, the strong biogeographic fidelity of *Cordylus,* and the fact that the range of *C. angolensis* occupies the same subregion as *C. machadoi* and *C. namakuiyus* **sp. nov.** (south-western Angola *sensu* Linder *et al.*, 2012), suggests that *C. angolensis* is more closely related to the Southern Angolan *Cordylus* species than to any of the Zambezian or Somalian species.

Acknowledgements

The authors acknowledge Dr. Soki Kuedikuenda, erstwhile director of the Instituto Nacional da Biodiversidade e Áreas de Conservação, for supporting the expeditions and issuing the necessary permits for collecting and exporting specimens; and thank the Secretary of Estate for Biodiversity of Angola, Dr. Paula Francisco, and the Minister of Environment, Dr. Fátima Jardim, for their institutional support. We thank our colleagues Jens Vindum, Ariana Kuhn, Sango de Sá, Werner Conradie, Krystal Tolley and Pedro vaz Pinto for their help in the field. We also thank David Kizirian, Lauren Vonnahme and Margaret Arnold for providing access to the specimens and field notes from the Vernay expedition, Anna Sellas for assistance with sequencing, and Megan Faillace for providing access to the Vtomex CT machine at the GE Inspection Technologies, LP Technical Solutions Center in San Carlos, California. Brian Huntley, Joao Serodio d'Almeida and the Traguedo family are acknowledged for organising the SANBI/ISCED/UAN 2009 Angolan Biodiversity Assessment and Capacity Building Project's faunal survey, and Bruce Bennett and the Baptista family are thanked for their logistical support during the 2013 fieldwork. Lauretta Mahlangu of Ditsong Natural History Museum (Pretoria) is thanked for the loan of specimens. Field surveys and analyses were supported by funds from award DEB 1202609 from the National Science Foundation to David Blackburn, the South African National Biodiversity Institute (SANBI), and the National Research Foundation of South Africa (NRF).

References

Bocage, J. (1895) *Herpétologie d'Angola et du Congo*. Imprimerie Nationale IXX: Lisbon, Lisbonne, 203 pp., 220 pls.

Branch, W.R. (1998) *Field guide to snakes and other reptiles of southern Africa.* Ralph Curtis Books Publishing: Sanibel Island, Florida, 399 pp.

Branch, W.R., Roedel, M.O. & Marais, J. (2005) A new species of rupicolous *Cordylus* Laurenti 1768 (Sauria: Cordylidae) from northern Mozambique. *African Journal of Herpetology*, 54, 131–138. http://dx.doi.org/10.1080/21564574.2005.9635526

Broadley, D.G. & Branch, W.R. (2002) A review of the small east African *Cordylus* (Sauria: Cordylidae), with the description of a new species. *African Journal of Herpetology*, 51, 9–34. http://dx.doi.org/10.1080/21564574.2002.9635459

Broadley, D.G. & Mouton, P.leF.N. (2000) A new species of rupicolous *Cordylus* Laurenti from Malawi (Sauria: Cordylidae). *African Journal of Herpetology*, 49 (2), 169–172
http://dx.doi.org/10.1080/21564574.2000.9635443

Conradie, W., Measey, G.J., Branch, W.R. & Tolley, K.A. (2012) Revised phylogeny of African sand lizards (*Pedioplanis*), with the description of two new species from south-western Angola. *African Journal of Herpetology,* 61 (2), 91–112.
http://dx.doi.org/10.1080/21564574.2012.676079

Edgar, R. (2004) MUSCLE: a multiple sequence alignment method with reduced time and space complexity. *BMC Bioinformatics*, 19 (113), 1–19.

Felsenstein, J. (1985) Confidence limits on phylogenies: an approach using the bootstrap. *Evolution*, 39, 783–791.
http://dx.doi.org/10.2307/2408678

Greenbaum, E., Stanley, E.L., Kusamba, C., Moninga, W.M., Goldberg, S.R. & Bursey, C.R. (2012) A new species of *Cordylus* (Squamata: Cordylidae) from the Marungu Plateau of south-eastern Democratic Republic of the Congo. *African Journal of Herpetology*, 61, 14–39.
http://dx.doi.org/10.1080/21564574.2012.666505

Haacke, W.D. (2008) A new leaf-toed gecko (Reptilia: Gekkonidae) from south-western Angola. *African Journal of Herpetology,* 57 (2), 85–92.
http://dx.doi.org/10.1080/21564574.2008.9635571

Huelsenbeck, J. & Ronquist, F. (2003) MrBayes: Bayesian Inference of Phylogeny. *Bioinformatics*, 17, 754–755.
http://dx.doi.org/10.1093/bioinformatics/17.8.754

Huntley, B.J. (2009) *SANBI/ISCED/UAN Angolan Biodiversity Assessment. Capacity Building Project. Report on Pilot Project March 2008 – February 2009*. Unpublished report, South African National Biodiversity Institute, Kirstenbosch, Cape Town, 1–111.

Kearse, M., Moir, R., Wilson, A., Stones-Havas, S., Cheung, M., Sturrock, S., Buxton, S., Cooper, A., Markowitz, S., Duran, C., Thierer, T., Ashton, B., Mentjies, P. & Drummond, A. (2012) Geneious Basic: an integrated and extendable desktop software platform for the organization and analysis of sequence data. *Bioinformatics*, 28 (12), 1647–1649.
http://dx.doi.org/10.1093/bioinformatics/bts199

Laurent, R. (1964) Reptiles et Amphibiens de l'Angola (Troisième contribution). — Companhia de Diamantes de Angola (Diamang). *Serviços Culturais*, Museu do Dundo (Angola), 67, 1–165.

Linder, H.P., de Klerk, H.M., Born, J., Burgess, N.D., Fjeldsta, J. & Rahbek, C. (2012) The partitioning of Africa: Statistically defined biogeographical regions in sub-Saharan Africa. *Journal of Biogeography*, 39, 1189–1205.
http://dx.doi.org/10.1111/j.1365-2699.2012.02728.x

Loveridge, A. (1944) Revision of the African lizards of the family Cordylidae. *Bulletin of the Museum of Comparative Zoology at Harvard College*, 95 (195), 1–118.

Marques, M. (2015) Geographical distribution of the amphibians and reptiles of Angola. Unpublished Msc Thesis, University of Évora, Alentejo – NUTSII, 684 pp.

Monard, A. (1937) Contribution à l'herpetologie d'Angola. Archos. *Museu Bocage (Lisboa)*, 8, 1–154.

Mouton, P. le F.N., Bates, M.F. & Whiting, M.J. (2014) Family Cordylidae. *In:* Bates, M.F., Branch, W.R., Bauer, A.M., Burger, M., Marais, J., Alexander, G.J. & de Villiers, M.S. (Eds.), *Atlas and red list of the reptiles of South Africa, Lesotho and Swaziland*. *Suricata. Vol. 1.* South African National Biodiversity Institute, Pretoria, pp. 182–223.

Nielsen, S.V. & Colston, T.J. (2014) The phylogenetic position of Ethiopia's sole endemic and biogeographically enigmatic cordylid lizard, *Cordylus rivae* (Squamata: Cordylidae), and a discussion of its conservation status. *African Journal of Herpetology*, 63 (2), 166–176.
http://dx.doi.org/10.1080/21564574.2014.953606

Nylander, J.A.A. (2008) MrModeltest 2.3. Program distributed by the author. Evolutionary Biology Centre, Uppsala University.

Stanley, E.L., Bauer, A.M., Jackman, T.R., Branch, W.R. & Mouton, P.leF.N. (2011) Between a rock and a hard polytomy: Rapid radiation in the rupicolous girdled lizards (Squamata: Cordylidae). *Molecular Phylogenetics and Evolution*, 58, 53–70.
http://dx.doi.org/10.1016/j.ympev.2010.08.024

Swofford, D.L. (2002) Paup* Phylogenetic Analysis Using Parsimony (and Other Methods) Version 4.0. ed. Sunderland, Massachusetts.: Sinauer Associates.

Wiens, J.J., Kuczynski, C.A., Townsend, T., Reeder, T.W., Mulcahy, D.G. & Sites, J.W. (2010) Combining Phylogenomics and Fossils in Higher-Level Squamate Reptile Phylogeny: Molecular Data Change the Placement of Fossil Taxa. *Systematic Biology*, 59, 674–688.
http://dx.doi.org/10.1093/sysbio/syq048

Zwickl, D.J. (2006) *Genetic algorithm approaches for the phylogenetic analysis of large biological sequence datasets under the maximum likelihood criterion*. Unpublished Ph.D. dissertation, The University of Texas, Austin, 115 pp.

SUPPLEMENTARY DATA

SUPPLEMENTARY DATA S1. Comparative material used in the description.

Cordylus namakuiyus: California Academy of Sciences: CAS 254912 (holotype), CAS 254754 (paratype), CAS 254755 (paratype), CAS 254913 (paratype), CAS 254914 (paratype), CAS 256529 (paratype), CAS 256530 (paratype), CAS 256531 (paratype), Port Elizabeth Museum: PEM R18005 (paratype), Ditsong Museum: TM 40430, American Museum of Natural History: AMNH 47274, AMNH 47275, AMNH 47276, AMNH 47277, AMNH 47278, AMNH 47279, AMNH 47280, AMNH 47281, AMNH 47282, AMNH 47283, AMNH 47284, AMNH 47285, AMNH 47286, AMNH 47287, AMNH 47288, AMNH 47289, AMNH 47290, AMNH 47291, AMNH 47292, AMNH 47293, AMNH 47294, AMNH 47295, AMNH 47296, AMNH 47297, AMNH 47298, AMNH 47299, AMNH 47300, AMNH 47301, AMNH 47302, AMNH 47303, AMNH 47304, AMNH 47305, AMNH 47306, AMNH 47307, AMNH 47308, AMNH 47309, AMNH 47310, AMNH 47311, AMNH 47312, AMNH 47313, AMNH 47314, AMNH 47315, AMNH 47316, AMNH 47317, AMNH 47318, AMNH 47319, AMNH 47320, AMNH 47321, AMNH 47322, AMNH 47323.

Cordylus machadoi (Angola): Museum of Comparative Zoology: MCZ R74120 (paratype), National Museum of Namibia, Windhoek: NMN 7002, Port Elizabeth Museum: PEM R*****, PEM R18006, PEM R18007, PEM R18008, PEM R18009, PEM R19782, PEM R19784, Ditsong Museum: TM 40095, TM 40096, TM 40131, TM 40132, TM 40133.

Cordylus machadoi (Namibia): Ditsong Museum:TM 57561

TABLE S2a. Voucher numbers and Genbank accession numbers for genetic samples.

Species	Voucher	Location	16S	12S	ND2
Cordylus aridus	PEMR16371	33°08’04”S, 22°32’20”E	HQ167169	HQ167058	HQ166958
C. beraduccii	JB6	Tanzania	KT941403	KT941400	KT941393
C. beraduccii	JB7	Tanzania	KT941404	KT941401	KT941394
C. beraduccii	WRB0037	07°07’58”S, 35°59’43”E	HQ167172	HQ167061	KT941395
C. cordylus	PEMR17466	34°11’43”S, 24°50’16”E	HQ167186	HQ167075	HQ166974
C. imkeae	MBUR01796	30°24’16”S, 18°06’06”E	HQ167198	HQ167087	HQ166986
C. jonesi	AMB8310	24°03’19”S, 28°24’13”E	HQ167199	HQ167088	HQ166987
C. jonesi	AMB8396	22°41’18”S, 29°31’16”E	HQ167200	HQ167089	HQ166988
C. machadoi	PEMR19784	14°57’42.7”S, 13°20’05.9”E	KT941141	KT941127	KT941257
C. machadoi	PEMR19782	14°57’42.7”S, 13°20’05.9”E	KT941142	KT941128	–
C. machadoi	PEMR18006	14°57’42.7”S, 13°20’05.9”E	KT941143	KT941129	–
C. machadoi	PEMR18007	14°57’42.7”S, 13°20’05.9”E	KT941145	KT941131	KT941259
C. machadoi	PEMR18008	14°57’42.7”S, 13°20’05.9”E	KT941144	KT941130	KT941258
C. machadoi	KTH09059	14°57’42.7”S, 13°20’05.9”E	KT941146	KT941132	KT941260
C. machadoi	PEMR18009	15°01’02.9”S, 13°19’15.2”E	KT941147	KT941133	KT941261
C. macropholis	AMB8874	32°06’37”S, 18°18’14”E	HQ167207	HQ167096	HQ166994
C. marunguensis	EBG2994	07º43'08.1"S, 29º45'52.4"E	JQ389803	JQ389798	KT941396
C. mclachlani	AMB8855	33°16’20”S, 19°37’42”E	HQ167208	HQ167097	HQ166995
C. meculae	PEMR16164	12º02’15”S, 37º38’19”E	HQ167210	HQ167099	–
C. meculae	PEMR16165	12º02’15”S, 37º38’19”E	HQ167211	HQ167100	–
C. meculae	PEMR16202	12º02’28”S, 37º37’21”E	HQ167233	HQ167122	–
C. namakuiyus	CAS254912	15º0'59.4"S, 12º38'31.3"E	KT941135	KT941121	KT941251
C. namakuiyus	CAS256529	15º0'59.4"S, 12º38'31.3"E	KT941136	KT941122	KT941252
C. namakuiyus	CAS254754	15º28'33.2"S, 12º27'45.7"E	KT941137	KT941123	KT941253
C. namakuiyus	CAS254755	15º28'33.2"S, 12º27'45.7"E	KT941138	KT941124	KT941254
C. namakuiyus	CAS256530	15º28'33.2"S, 12º27'45.7"E	KT941139	KT941125	KT941255
C. namakuiyus	CAS256531	15º28'33.2"S, 12º27'45.7"E	KT941140	KT941126	KT941256
C. namakuiyus	PEMR18005	15°59’48.5”S, 12°24’24.6”E	KT941148	KT941134	KT941262
C. niger	nigerSU1	32°59’04”S, 17°52’37”E	HQ167217	HQ167106	HQ167000
C. oelofseni	AMB8860	32°46’11”S, 18°42’10”E	HQ167221	HQ167110	HQ167004

.....continued on the next page

TABLE S2a. (Continued)

Species	Voucher	Location	16S	12S	ND2
C. oelofseni	CoeloSU1	34°02'24"S, 18°59'54"E	HQ167219	HQ167108	HQ167002
C. rhodesianus	ELSPET4	Pet trade: No locality	HQ167230	HQ167119	HQ167013
C. tropidosternum	JB8	Tanzania	KT941405	KT941402	KT941397
C. tropidosternum	WRB0042	Tanzania	HQ167235	HQ167124	KT941398
C. ukingensis	WRB0039	08°17'58"S, 35°40'43"E	HQ167237	HQ167126	KT941399
C. vittifer	AMB6073	26°08'00"S, 31°08'00"E	HQ167241	HQ167130	HQ167019
C. vittifer	AMB8274	24°31'49"S, 30°38'43"E	HQ167242	HQ167131	HQ167020
C. vittifer	AMB8603	25°18'11"S, 30°08'51"E	HQ167243	HQ167132	HQ167021
Namazonurus campbelli	MCZ27028	25°47'32"S, 16°25'31"E	HQ167174	HQ167063	HQ166962
Ouroborus cataphractus	MBUR01792	30°24'16"S, 18°06'06"E	HQ167177	HQ166965	HQ167066

TABLE S2b. Voucher numbers and Genbank accession numbers for genetic samples.

Species	Voucher	R35	NKTR	PRLR	KIF24
Cordylus aridus	PEMR16371	KT941314	KT941263	HQ167498	HQ167280
C. beraduccii	JB6	KT941315	KT941264	KT941390	–
C. beraduccii	JB7	KT941316	KT941265	KT941391	–
C. beraduccii	WRB0037	KT941317	KT941266	HQ167501	HQ167283
C. cordylus	PEMR17466	KT941318	KT941267	HQ167515	HQ167297
C. imkeae	MBUR01796	KT941319	KT941268	HQ167527	HQ167309
C. jonesi	AMB8310	KT941326	KT941275	HQ167528	HQ167310
C. jonesi	AMB8396	KT941327	KT941276	HQ167529	HQ167311
C. machadoi	PEMR19784	KT941328	KT941277	KT941306	KT941229
C. machadoi	PEMR19782	KT941329	KT941278	KT941307	KT941230
C. machadoi	PEMR18006	KT941330	KT941279	KT941308	KT941231
C. machadoi	PEMR18007	KT941332	KT941281	KT941310	KT941233
C. machadoi	PEMR18008	KT941331	KT941280	KT941309	KT941232
C. machadoi	KTH09059	KT941333	KT941282	KT941311	KT941234
C. machadoi	PEMR18009	KT941334	KT941283	KT941312	KT941235
C. macropholis	AMB8874	KT941336	KT941285	HQ167536	HQ167318
C. marunguensis	EBG2994	KT941337	KT941286	JQ389849	JQ389810
C. mclachlani	AMB8855	KT941338	KT941287	HQ167537	HQ167319
C. meculae	PEMR16164	KT941406	KT941409	HQ167539	HQ167321
C. meculae	PEMR16165	KT941407	KT941410	HQ167540	HQ167322
C. meculae	PEMR16202	KT941408	–	HQ167562	HQ167344
C. namakuiyus	CAS254912	KT941320	KT941269	KT941300	KT941223
C. namakuiyus	CAS256529	KT941321	KT941270	KT941301	KT941224
C. namakuiyus	CAS254754	KT941322	KT941271	KT941302	KT941225
C. namakuiyus	CAS254755	KT941323	KT941272	KT941303	KT941226
C. namakuiyus	CAS256530	KT941324	KT941273	KT941304	KT941227
C. namakuiyus	CAS256531	KT941325	KT941274	KT941305	KT941228

.....continued on the next page

TABLE S2b. (Continued)

Species	Voucher	R35	NKTR	PRLR	KIF24
C. namakuiyus	PEMR18005	KT941335	KT941284	KT941313	KT941236
C. niger	nigerSU1	KT941339	KT941288	HQ167546	HQ167328
C. oelofseni	AMB8860	KT941340	KT941289	HQ167550	HQ167332
C. oelofseni	CoeloSU1	KT941341	KT941290	HQ167548	HQ167330
C. rhodesianus	ELSPET4	KT941342	KT941291	HQ167559	HQ167341
C. tropidosternum	JB8	KT941343	KT941292	KT941392	KT941389
C. tropidosternum	WRB0042	KT941344	KT941293	HQ167564	HQ167346
C. ukingensis	WRB0039	KT941345	KT941294	HQ167566	HQ167348
C. vittifer	AMB6073	KT941346	KT941295	HQ167570	HQ167352
C. vittifer	AMB8274	KT941347	KT941296	HQ167571	HQ167353
C. vittifer	AMB8603	KT941348	KT941297	HQ167572	HQ167354
Namazonurus campbelli	MCZ27028	KT941349	KT941298	HQ167503	HQ167285
Ouroborus cataphractus	MBUR01792	KT941350	KT941299	HQ167506	HQ167288

TABLE S2c. Voucher numbers and Genbank accession numbers for genetic samples.

Species	Voucher	MYH2	RAG1	c-mos	BDNF
Cordylus aridus	PEMR16371	HQ167389	–	KT941186	KT941149
C. beraduccii	JB6	KT941386	KT941351	KT941187	KT941150
C. beraduccii	JB7	KT941387	KT941352	KT941188	KT941151
C. beraduccii	WRB0037	HQ167392	KT941353	KT941189	KT941152
C. cordylus	PEMR17466	HQ167406	KT941354	KT941190	KT941153
C. imkeae	MBUR01796	HQ167418	KT941355	KT941191	KT941154
C. jonesi	AMB8310	HQ167419	KT941362	KT941198	KT941161
C. jonesi	AMB8396	HQ167420	KT941363	KT941199	KT941162
C. machadoi	PEMR19784	KT941243	KT941364	KT941200	KT941163
C. machadoi	PEMR19782	KT941244	KT941365	KT941201	KT941164
C. machadoi	PEMR18006	KT941245	KT941366	KT941202	KT941165
C. machadoi	PEMR18007	KT941247	KT941368	KT941204	KT941167
C. machadoi	PEMR18008	KT941246	KT941367	KT941203	KT941166
C. machadoi	KTH09059	KT941248	KT941369	KT941205	KT941168
C. machadoi	PEMR18009	KT941249	KT941370	KT941206	KT941169
C. macropholis	AMB8874	HQ167427	KT941371	KT941208	KT941171
C. marunguensis	EBG2994	JQ389846	KT941372	KT941209	KT941172
C. mclachlani	AMB8855	HQ167428	KT941373	KT941210	KT941173
C. meculae	PEMR16164	HQ167430	KT941411	KT941413	KT941416
C. meculae	PEMR16165	HQ167431	KT941412	KT941414	KT941417
C. meculae	PEMR16202	HQ167453	–	KT941415	KT941418
C. namakuiyus	CAS254912	KT941237	KT941356	KT941192	KT941155
C. namakuiyus	CAS256529	KT941238	KT941357	KT941193	KT941156
C. namakuiyus	CAS254754	KT941239	KT941358	KT941194	KT941157

.....continued on the next page

TABLE S2c. (Continued)

Species	Voucher	MYH2	RAG1	c-mos	BDNF
C. namakuiyus	CAS254755	KT941240	KT941359	KT941195	KT941158
C. namakuiyus	CAS256530	KT941241	KT941360	KT941196	KT941159
C. namakuiyus	CAS256531	KT941242	KT941361	KT941197	KT941160
C. namakuiyus	PEMR18005	KT941250	–	KT941207	KT941170
C. niger	nigerSU1	HQ167437	KT941374	KT941211	KT941174
C. oelofseni	AMB8860	HQ167441	KT941375	KT941212	KT941175
C. oelofseni	CoeloSU1	HQ167439	KT941376	KT941213	KT941176
C. rhodesianus	ELSPET4	HQ167450	KT941377	KT941214	KT941177
C. tropidosternum	JB8	KT941388	KT941378	KT941215	KT941178
C. tropidosternum	WRB0042	HQ167455	KT941379	KT941216	KT941179
C. ukingensis	WRB0039	HQ167457	KT941380	KT941217	KT941180
C. vittifer	AMB6073	HQ167461	KT941381	KT941218	KT941181
C. vittifer	AMB8274	HQ167462	KT941382	KT941219	KT941182
C. vittifer	AMB8603	HQ167463	KT941383	KT941220	KT941183
Namazonurus campbelli	MCZ27028	HQ167394	KT941384	KT941221	KT941184
Ouroborus cataphractus	MBUR01792	HQ167397	KT941385	KT941222	KT941185

TABLE S3. Details of the X-ray conditions for CT scans of selected specimens.

Species	Accession #	Resolution µm	Voltage KV	Current mA	Capture time mS
C. namakuiyus **sp. nov.**	CAS 254912	69.13	100	200	333.3
C. namakuiyus **sp. nov.**	CAS 254913	40.00	70	220	333.3
C. namakuiyus **sp. nov.**	CAS 254914	40.00	70	220	333.3
C. namakuiyus **sp. nov.**	CAS 254754	68.58	100	150	333.3
C. namakuiyus **sp. nov.**	CAS 254755	68.58	100	150	333.3
C. namakuiyus **sp. nov.**	CAS 256529	31.57	100	150	333.3
C. namakuiyus **sp. nov.**	CAS 256530	50.11	110	140	333.3
C. namakuiyus **sp. nov.**	CAS 256531	74.68	140	120	500.0
C. namakuiyus **sp. nov.**	PEM R18005	71.68	140	150	333.3
C. namakuiyus **sp. nov.**	AMNH 47301	66.73	140	90	1000.0
C. machadoi	PEM R18006	75.58	140	150	333.3
C. machadoi	PEM R18009	43.64	110	150	333.3
C. machadoi	PEM R19782	66.40	140	150	333.3
C. machadoi	PEM R19784	57.67	140	150	333.3

TABLE S4. Loadings for principal component analyses using the complete and meristic only datasets. The largest loadings for each component are highlighted.

	Total dataset		Meristic only	
	PC1	PC2	PC1	PC2
Head length	**-0.370**	0.105	–	–
Dorsal transverse rows	**0.324**	0.039	-0.094	**0.278**
Tibia-fibular length	**-0.306**	-0.025	–	–
Head width	**-0.288**	0.008	–	–
Radius-Ulnae length	**-0.250**	0.043	–	–
Snout-Arm Length	**-0.218**	0.022	–	–
Longest toe length	**-0.217**	**0.291**	–	–
Transverse gulars	**0.216**	-0.133	**-0.330**	**0.278**
Ventral transverse rows	**0.214**	-0.080	-0.105	0.207
Snout-Eye Length	-0.198	0.097	–	–
Subdigital Lamellae T5	0.193	0.154	0.035	**0.309**
Head height	-0.163	0.157	–	–
Subdigital Lamellae F3	0.158	**0.323**	**0.249**	**0.295**
Dorsolateral longitudinal rows	0.155	**-0.194**	0.026	**0.295**
Subdigital Lamellae F5	0.153	0.251	0.150	0.210
Supralabiels	-0.133	-0.060	0.062	-0.093
Infralabiesl	0.132	**-0.206**	-0.191	0.258
Subdigital Lamellae F2	0.129	**0.337**	0.196	0.230
Chin shields	-0.126	-0.134	0.088	-0.057
Ventral longitudian rows	0.123	**-0.205**	0.213	0.179
Subdigital Lamellae T3	0.116	0.174	0.208	0.115
Axila-Groin Distance	0.114	0.094	–	–
Subdigital Lamellae T4	0.112	**0.337**	0.212	0.268
Femoral pores	0.097	-0.158	**-0.232**	0.181
Subdigital Lamellae T2	0.092	0.216	**0.310**	0.028
Preoculars	-0.070	-0.010	-0.072	-0.166
Loreal	-0.061	0.049	-0.053	-0.120
Suboculars	0.057	0.017	0.020	0.202
Subdigital Lamellae T1	-0.051	0.053	**0.271**	-0.008
Subdigital Lamellae F4	0.041	**0.347**	**0.462**	0.020
Femur length	-0.024	0.018	–	–
Subdigital Lamellae F1	0.010	0.201	0.143	0.135

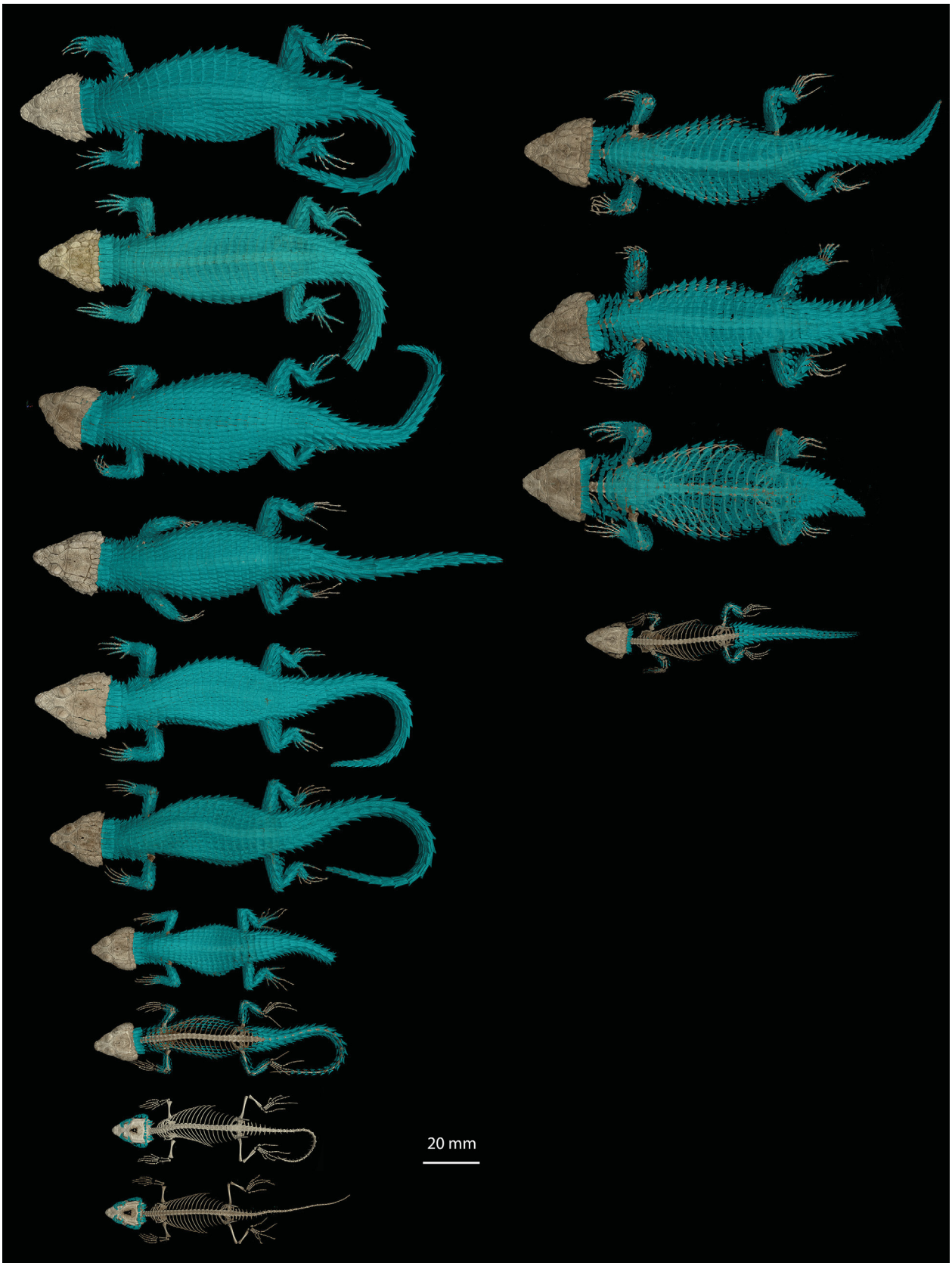

SUPPLEMENTARY FIGURE S1. ontogenetic variation in the osteoderm arrangements of *Cordylus namakuiyus* **sp. nov.** (left) and *Cordylus machadoi* (right). From top to bottom, *C. namakuiyus*: CAS 254912 (holotype), CAS 256531 (paratype), PEM R18005 (paratype), AMNH 472301, CAS 254755 (paratype), CAS 254754 (paratype), CAS 256530 (paratype), CAS 256529 (paratype), CAS 254913 (paratype), and CAS 254914 (paratype). *C. machadoi*: PEM R18006, PEM R19782, PEM R19784, and PEM R18009.

SUPPLEMENTARY FILES S2. Zipped .mov and .ply files of *Cordylus namakuiyus* **sp. nov.** holotype (CAS 254912) and paratype (CAS 254755) skeletons and osteoderms. The files can be downloaded here https://www.dropbox.com/s/2y5iy50twmngzxf/Stanley%20et%20al%20S2.zip?dl=0 and the .ply files viewed in any 3D model viewer, such as the freely available meshlab (www.meshlab.com).